The greenhouse gas budget of terrestrial ecosystems in East Asia since 2000

Xuhui Wang[1], Yuanyi Gao[1], Sujong Jeong[2], Akihiko Ito[3], Ana Bastos[4], Benjamin Poulter[5,6], Yilong Wang[7], Philippe Ciais[8], Hanqin Tian[9], Wenping Yuan[10], Naveen Chandra[11], Frédéric Chevallier[8], Lei Fan[12], Songbai Hong[1], Ronny Lauerwald[13], Wei Li[14], Zhengyang Lin[1], Naiqing Pan[15], Prabir K. Patra[11,16], Shushi Peng[1], Lishan Ran[17], Yuxing Sang[1], Stephen Sitch[18], Takashi Maki[19], Rona Louise Thompson[20], Chenzhi Wang[1], Kai Wang[1], Tao Wang[21], Yi Xi[1,8], Liang Xu[22], Yanzi Yan[1], Jeongmin Yun[23], Yao Zhang[1], Yuzhong Zhang[24,25], Zhen Zhang[26], Bo Zheng[27], Feng Zhou[1], Shu Tao[1], Josep G. Canadell[28], Shilong Piao[1]

[1]Institute of Carbon Neutrality, Sino-French Institute for Earth System Science, College of Urban and Environmental Sciences, Peking University, Beijing, China.

[2]Department of Environmental Planning, Graduate School of Environmental Studies, Seoul National University, Seoul, South Korea.

[3]National Institute for Environmental Studies, Tsukuba, Japan.

[4]Department of Biogeochemical Integration, Max Planck Institute for Biogeochemistry, Jena, Germany.

[5]Institute on Ecosystems and the Department of Ecology, Montana State University, Bozeman, Montana, USA.

[6]Biospheric Science Laboratory, NASA Goddard Space Flight Center, Greenbelt, USA.

[7]Key Laboratory of Land Surface Pattern and Simulation, Institute of Geographical Sciences and Natural Resources Research, Chinese Academy of Sciences, Beijing, China.

[8]Laboratoire des Sciences du Climat et de l'Environnement, LSCE/IPSL, CEA-CNRS-UVSQ, Université Paris-Saclay, France.

[9]Schiller Institute for Integrated Science and Society, Department of Earth and Environmental Sciences, Boston College, Chestnut Hill, USA.

[10]School of Atmospheric Sciences, SUN YAT-SEN University, Guangdong, China.

[11]Japan Agency for Marine-Earth Science and Technology (JAMSTEC), Yokohama, Japan.

[12]Chongqing Jinfo Mountain Karst Ecosystem National Observation and Research Station, School of Geographical Sciences, Southwest University, Chongqing, China.

[13]Université Paris-Saclay, INRAE, AgroParisTech, UMR ECOSYS, Thiverval-Grignon, France.

[14]Department of Earth System Science, Tsinghua University, Beijing, China.

[15]Schiller Institute for Integrated Science and Society, Department of Earth and Environmental Sciences, Boston College, Chestnut Hill, USA.

[16]Research Institute for Humanity and Nature (RIHN), Kamigamo, Kyoto, Japan.

[17]Department of Geography, The University of Hong Kong, Pokfulam Road, Hong Kong, China.

[18]Faculty of Environment, Science and Economy, University of Exeter, UK.

[19]Department of Atmosphere, Ocean and Earth System Modeling Research, Meteorological Research Institute, Japan Meteorological Agency, Tsukuba, Japan.

[20] NILU−Norsk Institutt for Luftforskning, Norway.

[21]Department of Civil and Environmental Engineering, The Hong Kong Polytechnic University, Hong Kong, China.

[22]Pachama, Inc. 2261 Market St #4303, San Francisco, USA.

[23]Jet Propulsion Laboratory, California Institute of Technology, Pasadena, USA.

[24]Key Laboratory of Coastal Environment and Resources of Zhejiang Province, School of Engineering, Westlake University, Hangzhou, China.

[25]Institute of Advanced Technology, Westlake Institute for Advanced Study, Hangzhou, China.

[26]Department of Geographical Sciences, University of Maryland, College Park, USA.

[27]Institute of Environment and Ecology, Shenzhen International Graduate School, Tsinghua University, Shenzhen, China.

[28]CSIRO Environment, Canberra, Australia.

Corresponding author: Xuhui Wang (xuhui.wang@pku.edu.cn)

Key Points:

- A comprehensive greenhouse gas (CO2, CH4 and N2O) accounting including about 40 flux terms over East Asia is reported.
- Terrestrial ecosystems in East Asia are close to greenhouse gas neutral.
- Natural ecosystems is a net greenhouse gas sink, compensated by a net source from agricultural ecosystems.

Abstract

East Asia (China, Japan, Koreas and Mongolia) has been the world's economic engine over at least the past two decades, exhibiting a rapid increase in fossil fuel emissions of greenhouse gases (GHGs) and has expressed the recent ambition to achieve climate neutrality by mid-century. However, the GHG balance of its terrestrial ecosystems remains poorly constrained. Here, we present a synthesis of the three most important long-lived greenhouse gases (CO_2, CH_4 and N_2O) budgets over East Asia during the decades of 2000s and 2010s, following a dual constraint bottom-up and top-down approach. We estimate that terrestrial ecosystems in East Asia is close to neutrality of GHGs, with a magnitude of between 196.9 ± 527.0 Tg CO_2eq yr^{-1} (the top-down approach) and -20.8 ± 205.5 Tg CO_2eq yr^{-1} (the bottom-up approach) during 2000-2019. This net GHG emission includes a large land CO_2 sink (-1251.3 ± 456.9 Tg CO_2 yr^{-1} based on the top-down approach and -1356.1 ± 155.6 Tg CO_2 yr^{-1} based on the bottom-up approach), which is being fully offset by biogenic CH_4 and N_2O emissions, predominantly coming from the agricultural sector. Emerging data sources and modelling capacities have helped achieve agreement between the top-down and bottom-up approaches to within 20% for all three GHGs, but sizeable uncertainties remain in several flux terms. For example, the reported CO_2 flux from land use and land cover change varies from a net source of more than 300 Tg CO_2 yr^{-1} to a net sink of ~-700 Tg CO_2 yr^{-1}.

1 Introduction

Over the past two decades, about 30% of anthropogenic CO_2 emissions have been absorbed by terrestrial ecosystems globally (Pierre Friedlingstein et al., 2022). Both atmospheric inversions and Dynamic Global Vegetation Models (DGVMs) show that the northern hemisphere contributes the most to the global land CO_2 sink (Stephens et al., 2007; Tagesson et al., 2020), but inconsistencies between the two approaches become larger since the turn of the century (P. Ciais et al., 2019). However, the northern hemisphere regions and carbon cycle components responsible for the discrepancies remain unclear. One hypothesis attributes part of the discrepancy to the world's largest ever afforestation in China (e.g., Chen et al., 2019, whose impacts on the carbon sink have not yet been well captured by current DGVMs used in global carbon budget assessments (S. Piao et al., 2018; Pugh et al., 2019; Yu et al., 2022; Yue et al., 2020). This also fuels recent debates on whether there is a stronger land CO_2 sink over East Asia than over the rest of northern hemisphere regions (S. Piao et al., 2022; J. Wang et al., 2020; Wang et al., 2022). The REgional Carbon Cycle Assessment and Processes, phase 2 (RECCAP-2) helps to fill the gap by providing consistent methodologies across all northern hemisphere regions and the rest of the world, with a GHG budget accounting effort focused on East Asia. This effort will help major countries in this region (China, Japan and Koreas) to assess and track the land CO2 sink in the pathways of achieving carbon neutrality.

Although CO_2 is the primary GHG responsible for global warming since the preindustrial era, the contribution of CH_4 and N_2O are appreciable, together they highly affect the climate system with global warming potentials that are 27 and 273 times greater than CO_2 at a 100 year time horizon (IPCC, 2021). The GHG budget, including CO_2, CH_4 and N_2O, is thus more relevant to assess the role of the terrestrial ecosystems in mitigating climate change. There is emerging evidence that terrestrial ecosystems could be a net source of GHGs due to emissions of CH_4 and N_2O from both natural and anthropogenic sources (H. Tian et al., 2016). This is

particularly the case for East Asia, given the high intensity of anthropogenic activities which may lead to emission of CH_4 and N_2O from ecosystems (e.g., high nitrogen fertilizer application rate (Xiaoqing Cui et al., 2021; H. Tian et al., 2020), high nitrogen deposition rate (G. Yu et al., 2019), large area of rice paddy fields (Zhang et al. 2016; Figure 1)). However, a knowledge gap remains to be filled in the net GHG budget of East Asia, undermining the region's ambition to manage the ecosystems for mitigating climate change.

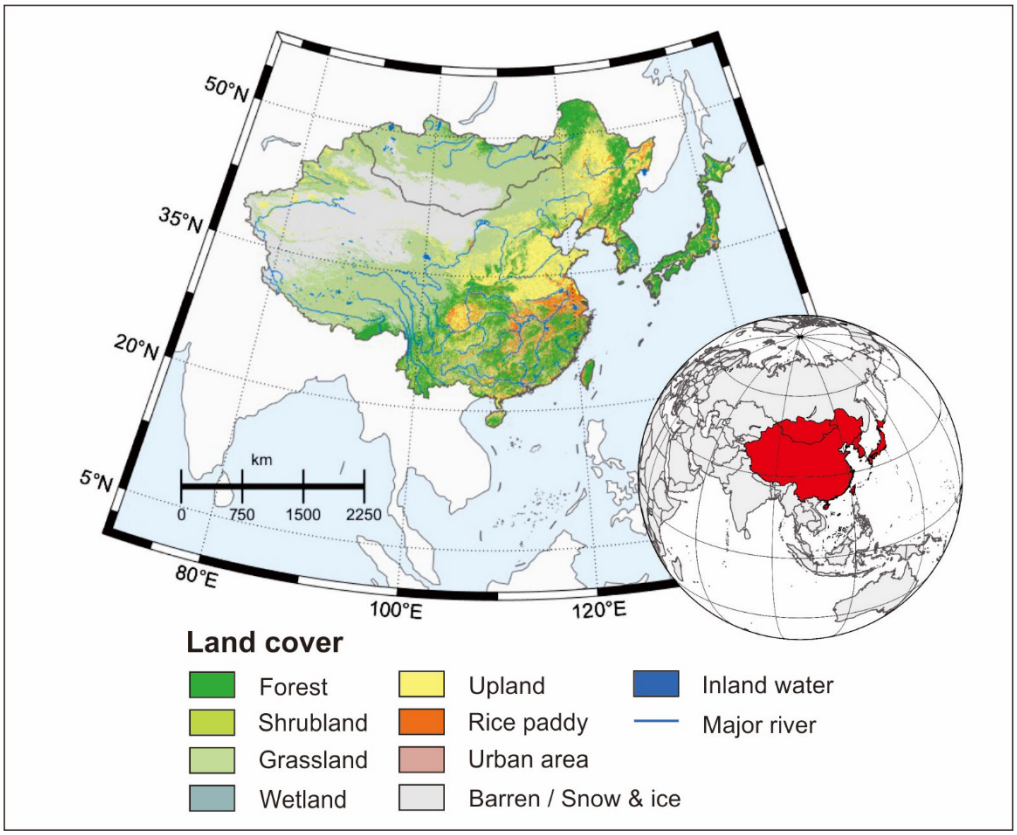

Figure 1. Geographical location and land cover type of East Asia.

In this study, we present a new assessment of the GHG budget of East Asia, with an accounting scheme following the guidelines of RECCAP-2 (Bastos et al., 2022; Philippe Ciais et al., 2022) and adapted to the regional characteristics and data availability in East Asia. The GHG budget is constrained both by observation-based assessments from inversions of atmospheric measurements of GHG mixing ratios ("top-down" approach hereafter) and by land-based assessments based on inventories and model simulations of carbon storage change and model estimates of GHG fluxes ("bottom-up" approach hereafter).

2 Methods

2.1 Study Area

Our study area focused on East Asia according to the RECCAP-2 regional division (Philippe Ciais et al., 2022), defined as the landmass including China, Japan, the Republic of Korea, the Democratic People's Republic of Korea, and Mongolia. The land area of East Asia is

~1.2×10^7 km^2, occupying ~8% of global land area. Ecosystems in this study include ecosystems such as forests, grasslands, shrublands, croplands, as well as wetlands and inland waters such as rivers, lakes and reservoirs.

2.2 Accounting framework of the GHG budget

The framework to assess the ecosystems GHG budget is adapted from the RECCAP-2 proposal (Philippe Ciais et al., 2022), which contains a set of shared and agreed definitions that are as precise as possible for each CO_2 flux to be reported. Compared to RECCAP-1, we aim to provide a synthesis of GHG budget for East Asia since 2000, including three major GHGs (CO_2, CH_4 and N_2O). We updated our accounting framework to GHG budget on the basis of carbon budget from Philippe Ciais et al. (2022), which is depicted in Figure 2.

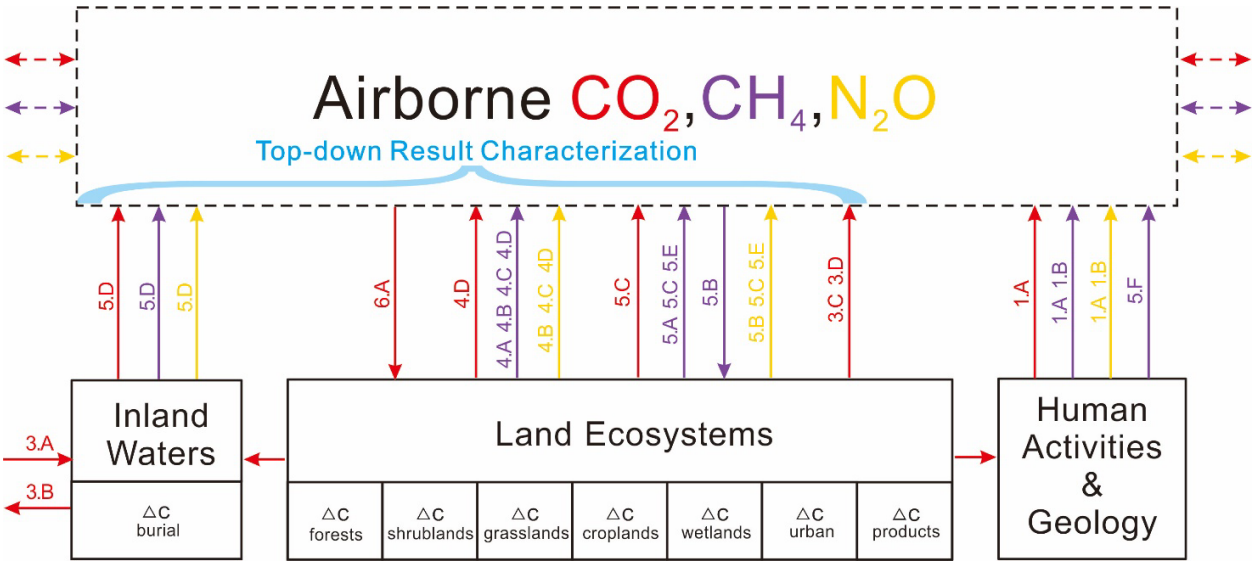

Flux Name			
1. Human activities	2.F Urban Construction	3.C Fossil Fuel RCC	5.B Natural Soil
1.A Fossil Fuel	2.G Burial	3.D Biogenic RCC	5.C Fires
1.B Waste and Landfill	2.H Wood Products	**4. Agriculture**	5.D Inland Waters
2. Carbon Stock Change	**NBP perspective**	4.A Enteric Fermentation	5.E Termites
2.A Forests	NBP	4.B Manure Management	5.F Geological Seepage
2.B Shrublands	Land Cover and Land Use Change	4.C Agricultural Soil	TD inversions
2.C Grasslands	**3. Lateral**	4.D Aqualculture	**Terrestrial Budget**
2.D Croplands	3.A Net Trade	**5. Other Sectors**	BU sink
2.E Wetlands	3.B Lateral Transport to Ocean	5.A Wetlands	TD sink

Figure 2. Accounting framework of the greenhouse gas balance with dual constraints. Flux terms included in the top-down approach indicated by the blue brace. Bottom-up estimates of the three greenhouse gas fluxes is shown in color arrows (CO_2 (red), CH_4 (purple), and N_2O

(yellow)). The horizontal arrow indicates lateral flux, and the vertical arrow indicates source/sink (upward/downward) of greenhouse gas to the atmosphere.

We recommend that our GHG budget is strictly speaking from ecosystems, the effect of fossil fuel combustion, cement production, industry, geological processes (e.g., volcanic eruption), waste and landfills (hereafter called "non-biosphere emissions" for simplicity) should be removed from the total budget. It can be captured by the top-down estimates of CO_2, CH_4, and N_2O flux excluding non-biosphere GHG emissions. The regional CO_2 budget includes CO_2 fluxes resulting from land cover and land use change, climate change and variability, rising atmospheric CO_2, biomass burning, and nitrogen deposition. Bottom-up approaches encompass various methods to quantify regional CO_2 budgets and their component fluxes. The CO_2 budget can be captured by the net carbon stock change of land ecosystems in a region (ΔC in Figure 2), which can be obtained by repeated measurements of live biomass, dead organic matter, soil carbon and by carbon stock change in wood and crop products. The CH_4 budget includes agricultural emissions produced by enteric fermentation, manure management, rice cultivation (included in 'agricultural soil' in our framework), aquaculture, and burning of crop residues. Other fluxes include emissions from fire, inland waters, natural wetlands, termites, as well as methane oxidation from natural soil. The N_2O budget includes those released from agricultural ecosystems, that is, fertilized soil emission, manure management, indirect N_2O emission from manure and synthetic nitrogen fertilizer use, and aquaculture. Sectors from natural ecosystems include emissions from natural soil, inland waters, as well from fire.

In assessing regional budgets, whether the budget components are well representative and accurate on the regional scale plays a more important role. Through the integration of data separately from bottom-up and top-down efforts with rigorous quantification of the uncertainties, we try to give a comprehensive synthesis of the terrestrial biogenic GHG budget for East Asia since 2000. The GHG fluxes and estimation methods are described in the following sections in detail.

In particular, we aim to perform a comprehensive review of available information together with newly produced data from in situ, space-based and data assimilation systems. Current gaps and weaknesses in knowledge and in monitoring systems are also considered in order to inform future requirements.

2.3 CO_2

2.3.1 Top-down approach

The top-down approach combines measurements of CO_2 mole fractions with atmospheric transport models in statistical optimization method (inversions) to constrain the magnitude and location of the combined total surface CO_2 fluxes from all sources, including fossil, land and ocean CO_2 fluxes (Pierre Friedlingstein et al., 2022). Inversions are rooted in Bayesian statistics with prior information on fluxes and their uncertainties. As the non-biosphere emissions (mainly fossil fuel emissions) of prior data are assumed to be well constrained, the atmospheric inversion is an effective method for quantifying the residual land-atmosphere CO_2 fluxes, although the fossil fuel emissions from East Asia may contain large errors which will contribute to errors in the biosphere fluxes from inversions (Jones et al., 2021; Saeki & Patra, 2017).

In this study, seven atmospheric inversions were used to infer the top-down estimates of the land–atmosphere CO_2 flux in East Asia. Five global state-of-the-art inversion systems from

the Global Carbon Budget (GCB) till 2019 (P. Friedlingstein et al., 2022) were used, including Copernicus Atmosphere Monitoring Service (CAMS) (Chevallier et al., 2005), Carbon-Tracker Europe (CTE) (Van Der Laan-Luijkx et al., 2017), Jena CarboScope (sEXTocNEET) (Rödenbeck et al., 2018), UoE (Feng et al., 2016) and CMS-Flux (Liu et al., 2021). They used very similar sets of surface measurements of CO_2 time series (or subsets thereof) from various flask and in situ networks. CAMS also used satellite xCO_2 retrievals from GOSAT and OCO-2 (Pierre Friedlingstein et al., 2022). As the primary goal of GCB was to provide a global scale estimate, some inversions may provide an unreasonable estimate regionally; therefore, we excluded the NISMON inversion (Niwa et al., 2017) because it estimated the northern hemisphere as land carbon source. In addition to the GCB inversions, the latest update of Japan Meteorology Agency CO_2 inversion system JMA (Maki et al., 2010) and the ensemble-based inversion system MIROC4-ACTM (N. Chandra et al., 2022) also provided data for this assessment.

For China, three inversions from Jiang et al. (2016), B. Chen et al. (2021), and Wang et al. (2022) using additional regional observations were also included. Jiang et al. (2016) and Chen et al. (2021) used two well-established inversion systems, respectively the nested Bayesian inversion (BI) system and the CarbonTracker-China (CTC) system, to estimate CO_2 fluxes in China. Weekly flask CO_2 measurements at regional background stations operated by China Meteorological Administration (CMA) are used in both systems. Jiang et al. (2016) estimated the CO_2 fluxes in China during 2006-2009 from three CMA sites (LFS, SDZ, and LAN) located in northeast China, north China, and east China, respectively. Chen et al. (2021) designed five inversions including different CMA sites (from 3 sites, including LFS, SDZ, and LAN to 7 sites, including LFS, SDX, LAN, WLG, SL, JS, and AKDL) to investigate the impacts of additional atmospheric CO_2 observations on estimate of the carbon sink in China during 2010-2013. The regional atmospheric inversions should be viewed with caution as the improper selection of sites may generally lead to serious representativeness error, Wang et al. (2022) carefully handled the representativeness error by performing a factorial analysis using the inversion system from CAMSv19 during 2010-2016, they quantified the biases of representing SL site observations in a coarse-resolution transport model and concluded that it could lead to extremely large inverse estimates. Their estimate eliminating the controversial site was used in this study. The final adjusted terrestrial CO_2 budget should subtract the net CO_2 flux from atmospheric oxidation of reduced carbon compounds (RCC). We estimated the net emissions from fossil fuel RCC (Ffrcc) and biogenic RCC (Fbrcc) based on Jiang et al. (2016) and the Global Fire Emission Database for biomass burning emission (GFED4s).

The fossil fuel induced CO_2 emissions estimated in this study followed the definition boundary described in the latest GCB (Pierre Friedlingstein et al., 2022), CO_2 emissions from the combustion of fossil fuels, industrial processes, chemical activities, and cement carbonation induced CO_2 uptake were estimated. We aimed to include all sources of fossil CO_2 emissions. The global inventory dataset CDIAC-FF (Gilfillan & Marland, 2021), which excludes emissions from lime production, the Emissions Database for Global Atmospheric Research (EDGARv7.0) from the European Commission Joint Research Centre (Crippa et al., 2022), and the PRIMAP-hist version 2.3.1 (Gütschow et al., 2021; Gütschow et al., 2016) were used in this study. We also used historical emissions from the CEDS (v2021_04_21) inventory (Hoesly et al., 2017; McDuffie et al., 2020), which was widely used in climate modelling. Regional specific datasets such as the Caron Emission Accounts and Datasets (CEADs) (Long et al., 2020; Shan et al., 2018; Shan et al., 2020) provided fundamental emission information for 30 emerging economies

including China and Japan, the national GHG inventories for China (NCCC, 2014, 2018) and Japan (NIES, 2022) were also taken into our estimation.

2.3.2 Bottom-up approach

2.3.2.1 Carbon stock change

The magnitude of the terrestrial CO_2 balance is driven by multiple processes, which can be quantified by the annual carbon stock changes (△C) (Luo et al., 2015). The △C in East Asia since 2000 were estimated as the sum of inventory-satellite-model based estimates from above-ground and below-ground carbon storage changes in different ecosystems pools. All the main types of ecosystems (forests, grasslands, croplands, others) and other natural carbon stocks (carbon burials in sediments and crop and wood products) are included. IPCC has published useful inventory methods for estimating GHG emissions, here, regionally distributed activity information and statistics are combined with technology-specific emission factors (EF). The methods are categorized into Tier 1, 2 or 3 approaches. Tier 1 represents the simplest approach that relies on default emission factors drawn from previous studies. Tier 2 and Tier 3 methods are based on more nuanced, nationally derived information, while Tier 3 could incorporate more sophisticated approaches, including models and temporally and spatially resolved activity data (IPCC, 2019).

Forests (△Cfor)

Forests cover ~14% of East Asia, contribute the main part of the carbon sink in terrestrial ecosystems. Our annual estimate of carbon stock change of forests (△Cfor) in East Asia is provided as the total amount from each East Asian countries. There were four regional datasets with detailed country-level information about △Cfor we included: three inventory-based estimates, FAO (Food and Agriculture Organization) Statistical reviews (FAO, 2021), the regional estimate published by Pan et al. (2011), an remote sensing estimate of aboveground live biomass (AGB) from L. Xu et al. (2021) and a model-based estimate from the OSCAR (Gasser et al., 2020). (1) FAO offered the country-level forests biomass carbon flux based on the activity data from FAO Forest Resources Assessments (FRA) in five-year cycles. (2) Pan et al. (2011) used the biomass expansion factors applied to convert volume estimates from inventory data of China (Fang et al., 2001), Japan (Fang et al., 2005), and Korea (Choi & Chang, 2004) to estimate △Cfor in East Asia during 2000-2007. (3) L. Xu et al. (2021) gave a new estimate for global AGB by synthesizing a large number of ground inventory plots (> 100,000) distributed mostly in boreal and temperate regions, airborne laser scanning (ALS) data across global tropical forests (>1 million ha), and satellite lidar inventory of global vegetation height structure (>8 million sample footprints) as a consistent set of measurements sensitive to forest structure and vegetation aboveground live biomass (AGB), and applied models relating the lidar-derived metrics and radar backscatter to AGB estimates. Considering the lack of below-ground biomass (BGB) estimate in L. Xu et al. (2021), we completed the BGB for this estimate by referring to the isometric growth rate of forests in China based on the observation-based result from Fang et al. (1996; $\frac{\mathrm{d}\log AGB}{\mathrm{d}\log BGB} = 0.96$). (4) OSCAR is a reduced-complexity model embedding a bookkeeping module as well as simplified biogeochemical process representation calibrated on dynamic

global vegetation models (DGVMs). It is not spatially resolved, but it is subdivided into country-level regions and 5 biomes.

Besides four regional datasets mentioned above, literature data that used national forest inventories or satellite-based method to calculate △Cfor for the subset region in East Asia were also taken into our consideration. For China, four extra estimates were also included. (1) The National Communication on Climate Change of The People's Republic of China (NCCC, 2010, 2018) provided △Cfor in China for 2005, 2010, 2012, and 2014 using the IPCC Tier 2 method. The △Cfor was estimated from different land types: high forest, bamboo, economic forest, sparse forest, and undeveloped afforested land. (2) Fang et al. (2018) presented an estimate for the mainland China since 2000 derived from the national climate-change research program, a 5-year Strategic Priority Project of Carbon Budget organized by the Chinese Academy of Sciences. Approximately 7,800 plots were sampled in forests across the country, using consistent research designs and protocols to investigate vegetation and soil carbon stock. (3) Jiang et al. (2016) reconstructed carbon stock changes of vegetation and soil in China during 2000s, the vegetation part was based on the 6th (1999–2003) and 7th (2004–2008) national forest inventories, three literature estimates were used as supplementary information. The soil part was calculated as the midpoint of the Integrated Terrestrial Ecosystem C-budget (InTEC) model and the inventory-based result from Pan et al. (2011). (4) Chang et al. (2023) used L-band Vegetation optical depth(L-VOD) product, retrieved from passive microwave satellite observations, to derive spatially explicit representations of changes in AGB during 2013–2019 across China. The result was extended to the total △Cfor (AGB+BGB) using the isometric growth rate method. The average and standard deviation from eight estimates were calculated to represent the regional △Cfor for China. For Japan, all forests are managed forests, and they consist of intensively managed forests, semi-natural forests, bamboo, and forests with less standing trees. The National Institute for Environmental Studies, Tsukuba (NIES, 2022) offered detailed △Cfor estimates from two land categories: "Forest land remaining Forest land" and "Land converted to Forest land" , according to the Forestry Status Survey [-FY2004] and the National Forest Resources Database (NFRDB) [FY2005-] (Forestry Agency). Another important estimate for Japan is based on the Survey on Forest Ecosystem Biodiversity by Japan Forest Agency. The estimate for biomass was aggregated by stand age and dominant species. For the dead wood, litter, and soil, the estimate was based on area-based expansion. A total of 6 estimates for Japan were available since 2000, the mean result was calculated in sector 3. For the Republic of Korea, an estimate using the national inventory data for different land types was added. For Mongolia, the extra estimate from L-VOD was also available. For the Democratic People's Republic of Korea, the mean result from the regional datasets was used.

Grasslands and Shrublands (△Cgra & △Cshr)

For China, similar to forests, the IPCC Tier 2 method adopted by NCCC and the model-based result from the OSCAR model were included to estimate the △C in grasslands and shrublands. Only the changes of soil organic carbon stock in grasslands were calculated in NCCC. Apart from these, S. Piao et al. (2009) developed a statistical function between the Global Inventory Monitoring and Modeling Studies (GIMMS) NDVI and aboveground biomass of grasslands and shrublands. The data material derived from the first national grassland resource survey across more than 2000 counties was conducted from 1981 to 1988 and 34 ecological research sites for shrubs. Fang et al. (2018) updated the newest estimate by combining field

311 measurements obtained from 5-y Strategic Priority Project of Carbon Budget with remote-
312 sensing data, about 4,030 plots from grasslands and 1,200 plots from shrublands were sampled in
313 ecosystem C sector: that is, vegetation biomass, dead organic matter, and soil organic carbon.
314 The BGB and total biomass were calculated using the ratios of belowground to aboveground
315 biomass for each grassland type and shrubland type obtained from expert judgments and
316 literature-review (Fang et al., 1996; Fang et al., 2018). For △Cgra and △Cshr of China, we used
317 the average of the above studies. For Japan, grasslands are generally covered with perennial
318 pasture and are mainly used for harvesting fodder or grazing. The NIES estimated the △Cgra
319 during the past 20 years. Carbon stock changes in five carbon pools: living biomass, dead wood,
320 litter, mineral soil and organic soil from three subcategories: pasture land, grazed meadow and
321 wild land are reported annually. It should be noted that the grasslands area is quite small in Japan
322 and △Cgra may be within the uncertainty range of △Cfor. An average of results from NIES and
323 OSCAR since 2000 was calculated for Japan. For the Republic of Korea, two estimates from the
324 national inventory data and OSCAR were used. For Mongolia and the Democratic People's
325 Republic of Korea, only the OSCAR estimate was available for grasslands and shrublands.

326 Croplands (△Ccro)

327 For croplands, biomass is subsequently harvested and used, releasing CO_2 back to the
328 atmosphere within less than a year (S. Piao et al., 2009), thus the biomass change in standing
329 crop are not taken into account in the carbon budgets. In this sector, the same method as the
330 △Cgra sector was used in each East Asian countries. For China, NCCC adopted the IPCC Tier 3
331 model method (Agro-C model) to calculate the change of soil carbon pool by simulating the
332 process of straw, roots and organic fertilizers entering the soil and leaving the soil through
333 decomposition. Piao et al. (2009) developed a statistical relationship between climate data
334 (temperature and precipitation), GIMMS NDVI data, and ground-based soil inventory data from
335 agricultural census during 1980s and 1990s. The estimate was updated when 4,060 soil sites
336 from croplands were sampled in the latest Strategic Priority Project of Carbon Budget (Fang et
337 al., 2018). For Japan, The NIES estimated △Ccro for the past 20 years. For the Republic of
338 Korea, Mongolia and the Democratic People's Republic of Korea, only the OSCAR estimates
339 were available.

340 Other ecosystems (△Coth)

341 Carbon fluxes in other ecosystems include carbon sink in wetlands and carbon emission
342 in urban areas. These sectors have been complied in the national inventory reports of China
343 (NCCC, 2010, 2018) and Japan (NIES, 2022) using the IPCC Tier 1-2 methods. OSCAR offered
344 the emission from urban areas for each country in East Asia.

345 Carbon burial in aquatic sediments (△Cburial)

346 Since there are widely distributed inland water bodies in East Asia, the amounts of
347 carbon that are transported to aquatic ecosystems and buried in the sediments of lakes and
348 reservoirs is considerable when compared to the carbon stock of land ecosystems. Three
349 estimates have been included to give a latest assessment for △Cburial in East Asia. (1) Jiang et
350 al. (2016) assumed that the carbon burial rate in Chinese lakes and reservoirs were about two
351 times of the global mean rate based on the previous studies of organic carbon burial rates in six

lakes in the middle and lower reaches of the Yangtze River Basin during 2000s (Gui et al. 2013, Dong et al. 2012). (2) Mendonça et al. (2017) compiled modern (last ~150 years) whole-basin OC burial data from the literature, and generated the OC burial in lakes and reservoirs in East Asia. (3) Wang et al. (2022) updated the △Cburial in China during 2010-2016 from Mendonca et al. (2017).

Harvest wood products (△Cpro)

Carbon accumulated in harvested wood products should be considered in the estimation of regional carbon budgets as it takes a long time before the wood products such as wooden furniture, building materials, etc., oxidize, emitting to CO_2 into the atmosphere. For China, we calculated the average △Cpro based on an inventory-based dataset and two literature estimates. (1) The NCCC offered an estimate for △Cpro in 2010 using the IPCC Tier 2 method. They applied the △Cpro in Europe (Janssens et al., 2003) and the ratio of wood products output between China and Europe based on FAO statistical databases. (2) Jiang et al. (2016) calculated the carbon pool changes of wood products due to local production in 2006–2009 using the production data of wood products from FAO statistical databases. For Japan, the annual carbon stock change in the harvested wood products pool has been evaluated in NIES since 1990 using IPCC Tier 2~3 methods.

2.3.2.2 Ecosystem modelling estimates

Net biome productivity (NBP)

NBP considers the carbon balance from the point of view of ecosystems and usually been quantified in process-based ecosystem models (Ciais et al. 2020). Spatially gridded NBP were obtained with simulation 2 (S2) from DGVMs up to 2019 from the TRENDY v9 dataset. 18 estimates have been provided in S2 from different DGVMs (CABLE-POP, CLASSIC, CLMS, DLEM, IBIS, ISAM, ISBA_CTRIP, JSBACH, JULES, LPJ-GUESS, LPJwsl, LPX-Bern, OCN, ORCHIDEE, ORCHIDEEv3, SDGVM, VISIT, YIBS). All the models are forced with observed climatology, atmospheric CO_2, time-invariant pre-industrial land-cover distribution and pre-industrial wood harvest rates, to model the contemporary global carbon cycle. It should be noted that the NBP we estimated from TRENDY models did not consider the changes in land use and land management explicitly.

Land cover and land use change flux (Fluc)

The net CO_2 flux from land cover, land use change, and forestry (Fluc) includes CO_2 fluxes from deforestation, afforestation, logging and forest degradation (including harvest activity), shifting cultivation (cycle of cutting forest for agriculture, then abandoning), and regrowth of forests (following wood harvest or agriculture abandonment) (Pierre Friedlingstein et al., 2022). It is extremely challenging to accurately estimate the carbon balance change associated with land-use change because of current lack of information on the spatial pattern of deforestation and associated changes in biomass and soil carbon stocks (Houghton, 2007; Shilong Piao et al., 2009). Six estimates, including three bookkeeping approaches, the updated estimates from BLUE (Hansis et al., 2015), OSCAR (Gasser et al., 2020), and H&N2017 (Houghton & Nassikas, 2017); three data-based or model-based approaches, an average estimate

derived from 18 dynamic global vegetation models (TRENDY), an estimate based on the latest Chinese forests land cover dataset by Yu et al. (2022) and a process-based model estimate driven by high resolution satellite land cover maps (Leng et al., under review) were used to estimate the net flux of Fluc in East Asia. Considering the TRENDY models and Hansis et al. (2015) were driven by a common land use forcing LUH2 (Chini et al., 2021), which contradicted ground-based and satellite evidence of land cover change in China (e.g. Yu et al. 2022) by showing increasing cropland area and decreasing forest area, we took the average from H&N2017, OSCAR, Yu et al. (2022) and Leng et al. (under review). For Japan, the Republic of Korea, Mongolia and the Democratic People's Republic of Korea, all six datasets estimates have been used.

2.3.2.3 Lateral fluxes

Wood and food trade (Ftrade)

Ftrade is the net lateral flux of crop and wood products related to trade across the boundaries of each region, calculated as the sum of the export and import fluxes of crop and wood products. For East Asia, we referred to the estimate from Ciais et al. (2021). They estimated the lateral flux of crop products based on the FAO database and Peters et al. (2012) for different forestry products for 2000s. For China, in a similar manner, Wang et al. (2022) updated the value during 2010-2016. Jiang et al. (2016) estimated the Ftrade based on the import and export data of crop and wood products from the FAO statistical databases. We calculated the average of the two estimates mentioned above to represent Ftrade flux in China.

Carbon export by rivers (Fexport)

The river export of carbon delivered to the ocean and across the boundaries of the region includes dissolved organic carbon (DOC), dissolved inorganic carbon (DIC) and particulate organic carbon (POC). For East Asia, RECCAP-1 estimated the lateral export of carbon involved in terrestrial biological carbon cycling (i.e. excluding the inputs from mineral dissolution given by the difference DIC-DICuptake by chemical rock weathering). The DOC and POC were derived from GlobalNEWS2 (Mayorga et al., 2010), DIC and DICatm (it represents the CO_2 uptake by chemical rock weathering) were derived from Hartmann et al. (2009).

For China, we calculated the mean result from three different methods. (1) We used the RECCAP-1 estimate mentioned above. (2) We used the estimate from Jiang et al. (2016) that based on the observations and empirical formula from previous studies, they estimated Fexport of nine Chinese exorheic rivers during 2006-2009. (3) We used a recent data-driven model estimate (Yan et al. under review) of DOC export from land to oceans, which applied machine learning methods and a comprehensive set of natural and anthropogenic drivers. Based on Yan et al.'s estimate and the mean DIC/DOC and POC/DOC ratios observed in the nine rivers from Jiang et al. (2016), we calculated the total carbon exported through the southeast boundaries of East Asia.

2.3.2.4 Other Natural Sectors

Inland waters outgassing (Fwater)

The flooding of large stocks of terrestrial organic matter into inland waters may fuel microbial decomposition, converting the organic matter stored in above and below ground biomass to CO_2. The CO_2 outgassing from inland waters in East Asia is calculated in four types of waters: rivers, natural lakes (lake type 1), reservoirs (lake type 2) and lakes regulated by dam (lake type 3). For East Asia, 11 global literature estimates (detailed information in Table S1) have been synthesized in RECCAP-2, all fluxes are rescaled to consistent estimates of surface area of lakes and reservoirs (after HydroLAKES, Messager et al. (2016)) and rivers (Allen & Pavelsky, 2018). They were further corrected for effects of seasonal ice-cover and ice out (Lauerwald et al. submitted).

Fire CO_2 emissions (Ffire)

Two datasets of carbon emissions from fire were collected in our study, the fourth version of the Global Fire Emissions Database (GFED4.1s, van der Werf et al. (2017)) and the Live Vegetation Biomass Carbon for the 21st Century (LVBC, Xu et al., 2021) . GFED4.1s combined satellite information on fire activity and vegetation productivity to estimate gridded monthly burned area and fire emissions of different fire types: boreal forest fires, temperature forest fires, tropical forest fires, peat fires and agricultural waste burning. LVBC made a conservative estimate of fire emissions separately for forest and non-forest areas by combining Landsat-based forest cover change product and the Moderate Resolution Imaging Spectroradiometer (MODIS) burned area product to avoid the overestimation in confusing the partial clearing from fire with the total clearing in Landsat forest cover change algorithm. We calculated the average of these two estimates for East Asia during 2000-2019.

2.4 CH_4 and N_2O

2.4.1 Top-down inversions

For CH_4, we included seven global inversions as described in GCP (Saunois et al., 2020). These inversions were performed for periods during 2000-2017 using surface and/or satellite observations. Satellite GOSAT retrievals were available only after 2009. Our study also included the updated MIROC4-ACTM (Naveen Chandra et al., 2021) and CAMS v20r2_surface inversion results (Arjo et al., 2020). In addition to satellite and surface data that have been assimilated in the above global inversions, we also included results from a regional inversion by Y. Zhang et al. (2022) who additionally assimilated surface methane measurements from 7 CMA sites across China. They quantified methane emissions during 2010-2017 in East Asia and found that these new data improved the constraints on methane emissions at the sub-regional level. The non-biosphere emissions (induced from fossil fuel, geology, waste and landfills) were subtracted in our final top-down estimate (see equation (2)).

For N_2O, as described in Tian et al. (2020) a total of four estimates from four independent atmospheric inversion frameworks were used in GCP, including GEOSCHEM, INVICAT, MIROC4-ACTM, PyVAR_CAMS. The latest versions which go extend until to 2019 were used in this study. The signal from fossil fuel emissions was removed at the post-processing stage

from the inversions mentioned above. We additionally removed the emissions from waste and landfills. The average result (including emissions from natural ecosystems and agricultural ecosystems) from the above five estimates since 2000 has been calculated for East Asia.

For the CH_4 and N_2O emissions from fossil fuel and industry, the latest versions of three global datasets: EDGAR, CEDS and PRIMAP-HIST were used to estimate emissions related to fossil fuel and industry. National inventories the NCCC for China and the NIES for Japan were also included. Non-CO_2 emissions from waste and landfills includes emissions from managed and non-managed landfills (solid waste disposal on land), and wastewater handling, where all kinds of waste are deposited (Saunois et al. 2020). Data from four global inventories were taken into consideration for East Asia (CEDS, GAINS, EDGAR, PRIMAP-HISP), country-level estimates from NCCC and NIES were also included.

2.4.2 Bottom-up methods

2.4.2.1 Agriculture

While agriculture sectors include a large variety of activities, in practice these sectors were categorized into emissions from enteric fermentation (only CH_4 emissions), manure management, agricultural soils (CH_4 emissions mainly from rice paddies and N_2O emissions mainly from upland soils) and aquaculture.

Enteric fermentation (Fenteric)

CH_4 emissions from enteric fermentation accounts for the majority (~90%) of global CH_4 emissions from livestock (Caro et al., 2014; Kumari et al., 2020; Tubiello, 2019). Ruminants represent the main source of the emissions in most countries, especially for China and Mongolia, this flux would be substantial. Three global emission inventories, one regional inventory, and available national inventory reports have been used in this study. The global estimates included FAOSTAT (2021), the EDGARv7.0 (Crippa et al. 2022), and CEDS (v2021_04_21) (Hoesly et al., 2017; McDuffie et al., 2020). The above three inventories are derived using a bottom-up approach where emissions are estimated using reported activity data and source- and region-specific (where available) emission factors. (1) FAOSTAT jointly disseminates the emissions reported by countries to the United Nations Framework Convention on Climate Change (UNFCCC). Estimates are computed at Tier 1 following the IPCC Guidelines for National GHG Inventories from activities located within FAO. (2) EDGAR follows the IPCC (2006) methodology, with FAO (2021) crop and livestock data, specified as livestock numbers for buffalo, camels, dairy and non-dairy cattle, goats, horses, swine, sheep, mules, asses and poultry (turkeys, geese, chickens and ducks). The livestock populations and cultivated areas rely on FAO (2021) activity data are further disaggregated according to different technologies and processes. Where available, nationally, regionally or tailored technology based on Tier 2 emission factors are implemented in EDGAR, and in their absence, default Tier 1 emission factors from IPCC guidelines (IPCC, 2006, 2019) are used. (3) CEDS aims to improve upon existing inventories with a more consistent and reproducible methodology applied to all emissions species, updated emission factors, and recent estimates from 1960 through 2019 (Hoesly et al., 2017; McDuffie et al., 2020). It implements a process whereby default emissions were taken directly from national inventories, gap-filled over time using EDGAR estimates with population data from United Nations (UN). CH_4 emissions from enteric fermentation are estimated in nine livestock species:

cattle, buffalo, sheep, goats, camels, horses, asses, and swine. For East Asia, L. Zhang et al. (2021) estimated CH_4 emissions from ten categories of livestock in East Asia during 1961 ~ 2019 following the Tier 2 approaches suggested by the 2019 Refinement to the IPCC 2006 Guidelines. For China and Japan, the national GHG reports NCCC and NIES were also collected, respectively.

Manure management (Fmanure)

In the case of nonruminant CH_4 emissions, there are about 970 million domestic swine in the world, and nearly half of them are in China (FAO, 2021). The large swine population produces considerable amounts of CH_4 emissions through manure production and management processes (P. Xu et al., 2019; L. Zhang et al., 2021). We synthesized the estimates from the latest CEDS, EDGAR and FAOSTAT datasets and Zhang et al. (2021a) for this sector.

N_2O emissions from livestock mainly derived from manure management, including livestock excretion, outdoor/grazing, housing, storage, treatment and field application, are considered to produce N_2O. In addition to the datasets mentioned above, here we also used a combination of datasets, the Potsdam Real-time Integrated Model for probabilistic Assessment of emissions Paths (PRIMAP-HIST) emission series (Gütschow et al., 2016). The PRIMAP-HIST dataset combined several published datasets to create 2 comprehensive sets (HISTCR and HISTTP) of GHG emission pathways from the years 1850 to 2018. Different priorities are given depending on the data types. In HISTCR scenario, country-reported data (CRF, BUR, UNFCCC) is prioritized over third party data (CDIAC, FAO, Andrew, EDGAR, BP). In HISTTP scenario, third-party data (CDIAC, FAO, Andrew, EDGAR, BP) is prioritized over country-reported data (CRF, BUR, UNFCCC). Both of the sets were used in this study. For country-scale estimates, in addition to the national GHG report NCCC for China and NIES for Japan, we included an estimate made for China from P. Xu et al. (2022), which used the NUtrient flows in Food chains, Environment and Resources use (NUFER) model and the principle of mass balance method with county-level activity data and N_2O emissions from 1978 to 2016 from province-level activity data and province-specific EFs. This estimate is close to the IPCC Tier 3 approach. Four models (DELM, ORCHIDEE, ORCHIDEECNP, VISIT) simulation results from NMIP project (Hanqin Tian et al., 2018) were also used in this study.

Agricultural soils (Fagri_soil)

Rice cultivation is a major source of CH_4 as most of the world's rice is grown in flooded paddy fields (Qiu, 2009). The estimates of CH_4 emissions from agricultural soils in this study were obtained from five inventory results (the latest CEDS, EDGAR, FAOSTAT, PRIMAP-HISP and The U.S. Environmental Protection Agency (EPA, 2021)), and two model estimates from VISIT are considered for the comparative purpose. EPA provides non-CO_2 GHG emissions based on a Tier 1 methodology. Activity data for rice cultivation included rice area harvested from the latest FAO (2021), type of water management regime and rice-growing season length from GRiSP (*GRiSP (Global Rice Science Partnership) Rice Almanac.*, 2013), and growth rate of rice area harvested from IFPRI's IMPACT model (2017). Several country-level estimates such as NCCC and NIES for China and Japan respectively were also selected as estimates for each country in East Asia.

552 N_2O emission from agricultural soils associated with fertilizer, crop residues, and other N
553 additions to soils are captured. Both direct and indirect agricultural soil emissions need to be
554 considered. It is primarily (more than half) attributable to the increase of fertilizer input to
555 uplands (Ito et al., 2018). Here we calculated this flux based on a common approach, outlined by
556 Bouwman (1996), in which direct soil N_2O emissions are calculated as the sum of emissions
557 caused by anthropogenic fertilizer-induced emissions plus the remaining background emissions,
558 and the indirect emissions from N volatilization/deposition and N leaching. Data for East Asia
559 was obtained as the ensemble mean of N_2O emissions from six estimates (the latest CEDS,
560 EDGAR, FAOSTAT, PRIMAP-HIST, EPA, and X. Cui et al. (2022)), six available model
561 results from NMIP were used. Different from using the Tier 1 methodology as most of the global
562 inventories, Cui et al. (2022) provided a Tier 3 estimate using a linear mixed-effect model and
563 survey-based data set of agricultural management measures to quantify the spatiotemporal
564 changes of crop-specific cropland-N_2O emissions from China between 1980 and 2017.

565 Aquaculture (Faquaculture)

566 Aquaculture systems might be potential hotspots for GHG emissions because they have
567 higher biological density and enrichment from fertilizer and feed compared with natural aquatic
568 ecosystems. China is the largest aquaculture producer globally, so errors from omitting in other
569 East Asia countries are expected to be small. In this study, we focused on the emissions from
570 aquaculture in China due to data limitations.

571 The CH_4 fluxes from aquaculture was acquired from two latest comprehensive studies
572 (Dong et al., 2023; Yifei Zhang et al., 2022). Zhang et al. (2022) presented a nationwide
573 metadata analysis from 132 aquaculture sites in China based on 62 published papers. Four land-
574 based aquaculture systems were taken into account, including the coastal wetland reclamation
575 system (CWRS), inland pond system (IPS), lake/reservoir system (LRS) and rice-field system
576 (RFS). Dong et al. (2023) analyzed the CH_4 emissions from aquaculture ponds in China with a
577 database of 55 field observations, which corresponds to the emissions from IPS ecosystems.

578 East Asia contributed 71%–79% of global aquaculture N_2O emissions (Tian et al. 2020).
579 The N_2O emissions were estimated from three different methods for the past 20 years (Hu et al.,
580 2012; H. Tian et al., 2020; Zhou et al., 2021). Hu et al. (2012) summarized the nitrogen
581 transformation mechanisms of N_2O production and suggested the average N_2O emission factor of
582 aquaculture system is 1.69 g N_2O−N/kg fish globally. We made a rough Tier 1 estimate for East
583 Asia based on this default emission factor by multiplying it with aquaculture production data
584 from FAOSTAT(2022). Using a Tier 2 methodology, Zhou et al. (2021) quantified N_2O emission
585 from Chinese aquaculture systems since the Reform and Opening-up (1979–2019) at the species-
586 , provincial-, and national- levels using annual aquaculture production data, based on nitrogen
587 (N) levels in feed type, feed amount, feed conversion ratio, and emission factors. Tian et al.
588 (2020) provided a comprehensive estimate for the period 2007-2016 with their meta estimate and
589 a nutrient budget model estimate. For Japan, the high consumption of fish is a feature of the
590 Japanese diet (Oita et al., 2018). Hayashi et al. (2021) noticed a high nitrogen use efficiency
591 (NUE) is obtained by fish production due to wild-catch fish, and they estimated the N_2O
592 emission of fish farming area in Japan from 2000 to 2015 to be 0.16~0.31 Gg N_2O yr^{-1} by using
593 the fate factors of surplus N as 1.25%.

2.4.2.2 Other Sectors

Wetlands methane emission (Fwet)

CH_4 emissions from wetland in this study were mainly derived from the Global Methane Budget (GMB) (Saunois et al., 2020). The GMB provides estimates for East Asia from 13 process-based models during 2000-2017. The dataset WetCHARTs (Bloom et al., 2017) provides global monthly wetland CH_4 emissions and uncertainty from an ensemble of multiple terrestrial biosphere models, wetland extent scenarios, and CH_4:C temperature dependencies. The intended use of the products is as a process-informed wetland CH4 emission and uncertainty data set for atmospheric chemistry and transport modelling. Here we used the result from WetCHARTs for the comparative purpose.

Inland waters outgassing (Fwater)

We synthesized CH_4 and N_2O emissions from three types of inland water bodies (includes rivers, natural lakes, reservoirs, lakes regulated by dams) in East Asia. Because the estimates for inland waters are difficult to measure continuously, we assumed that the values are constant during 2000-2019. For CO_2 we obtained estimates from 10 studies whose study period covers the past 20 years. For CH_4 and N_2O, we obtained from 8 studies and 5 studies, respectively (detailed information in Table S2, S3).

Fire CH_4 and N_2O emissions (Ffire)

Similar to the CO_2 emissions from fires, we used GFEDv4.1s (van der Werf et al. 2017) to estimate CH_4 and N_2O emissions in this sector. Emissions of five different fire types were considered.

Natural soil CH_4 sink and N_2O source (Fnatu_soil)

Oxidation of atmospheric CH_4 by methanotrophs in natural soils and N_2O emissions from unmanaged soil were evaluated by the process-based terrestrial ecosystem model VISIT (Ito et al., 2018), which contained four schemes for simulating the process. Results from simulating natural vegetation and croplands separately at each grid were used. The output data was at 0.5° × 0.5° resolution and a timeseries between 2000-2016 was extracted for our estimation.

Termites CH_4 emission (Ftermite)

Termites are known as a CH_4 source (Ito et al., 2019), which is related to symbiotic cellulose-digesting microbes in their digestive tracts. Given the difficulty in mapping the regional distribution of termites, our estimate was simply based on the conventional empirical estimation after Ito et al. (2019) who used land-use data and emission factors from the literature.

2.5 Calculation of net GHG budgets

We then tried to make top-down and bottom-up results comparable through lateral flux adjustments for each greenhouse gas following the formula below:

$$\mathrm{TD}_{\mathrm{CO_2}} = \text{inversion } \mathrm{CO_2} \text{ flux} + \mathrm{F_{frcc}} + \mathrm{F_{brcc}} + \mathrm{F_{trade}} \quad (1)$$

$$TD_{CH_4}{}^{a} = \text{inversion } CH_4 \text{ total source} - F_{fossil}{}^{b} - F_{waste}{}^{c} - F_{geology}{}^{d} \quad (2)$$

$$TD_{N_2O} = \text{inversion } N_2O \text{ source} - \text{Fwaste} \quad (3)$$

$$BU_{CO_2} = \Delta C_{forest} + \Delta C_{grassland} + \Delta C_{cropland} + \Delta C_{other} + \Delta C_{burial} + \Delta C_{product} + F_{export} \quad (4)$$

$$BU_{CH_4} = F_{enteric} + F_{manure} + F_{agrisoil} + F_{aqua} + F_{wetland} + F_{natusoil} + F_{fire} + F_{water} + F_{termite} \quad (5)$$

$$BU_{N_2O} = F_{manure} + F_{agrisoil} + F_{aqua} + F_{natusoil} + F_{fire} + F_{water} \quad (6)$$

Note: [a]Top-down budget: the fossil fuel emission is assumed to be well constrained at pre- and post-processing stage from CO_2 and N_2O inversions, but not removed from CH4 inversions. [b]Ffossil: fossil fuel induced GHG emissions (data reference: CDIAC-FF Gilfillan and Marland et al. 2021). [c]Fwaste&landfill: waste treatments and landfills induced emissions (data reference: CEDS, EDGAR, IIASA GAINS and PRIMAP. [d]Fgeology: geological seepage induced CH_4 emissions (data reference: Etiope et al., 2019).

The total influence of three greenhouse gases was calculated separately for bottom-up and top-down approaches. GWP100 and GWP20 (global warming potentials on 100-year or 20-year time horizon) were used to indicate integrated radiative forcing of CH_4 and N_2O in terms of a CO_2 equivalent unit. We adopt 100-year GWPs of 27.0 and 273 for CH_4 and N2O, 20-year GWPs of 79.7 and 273 for CH_4 and N_2O refer to IPCC AR6 Table 7.15 (Canadell et al., 2021), respectively. The final terrestrial ecosystem GHG budget for the three main GHG gases was calculated by applying the following equation (Figure 4):

$$GHG = Budget(CO_2) + Budget(CH_4) * GWP_{CH_4} + Budget(N_2O) * GWP_{N_2O} \quad (7)$$

2.6 Uncertainty estimates

Uncertainty in the total budget for each greenhouse gas was obtained by error propagation from uncertainties of each term from equation (1) to equation (6), which is independent of each other. Most of the terms corresponding to the above fluxes had more than 1 estimate from different sources. The standard deviation of different estimates over the past 20 years was calculated at the national scale, and it is used to quantify uncertainty. As for the other fluxes which only involved one single estimate, the reported uncertainty for each estimate was considered as the uncertainty of this term.

3 Results and Discussions

3.1 CO_2 budget

3.1.1 Top-down

An ensemble of seven atmospheric inversion models and three inversions using additional regional observations estimated East Asia to have a net land-to-atmospheric CO_2 flux of -1515.3 ± 450.1 Tg CO_2 yr^{-1} (Table 1), ranging from -662.5 Tg CO_2 yr^{-1} to -1786.8 Tg CO_2 yr^{-1}. According to the seven global atmospheric inversions, this accounts for 18% of global land CO_2 sink. We adopted three regional inversions (Jiang et al. 2016, Chen et al. 2021, Wang et al. 2022), which used latest available CO_2 measurements by Chinese Meteorological Administration not included in the global inversions. These regional inversions did not show significant

differences with the global inversions for East Asia's land CO_2 sink. By adjusting for the CO_2 fluxes induced by lateral C transport processes (net trade of food and wood products, reduced carbon compounds of fossil fuel and biogenic sources) (Ciais et al. 2019, Wang et al. 2022), the terrestrial ecosystem over East Asia is a net sink of CO_2 by -1251.3 ± 456.9 Tg CO_2 yr^{-1}.

Table 1. The GHG budget in East Asia since 2000.

Sectors		**CO_2 (Tg CO_2 yr^{-1})**		**CH_4 (Tg CH_4 yr^{-1})**		**N_2O (Tg N_2O yr^{-1})**	
		Mean	**Uncertainty**	**Mean**	**Uncertainty**	**Mean**	**Uncertainty**
1. Human Activities	1.A Fossil Fuel	9493.35	221.83	23.40	1.90	0.58	0.05
	1.B Waste and Landfill			11.38	3.20	0.32	0.48
	Subtotal	9493.35	221.83	**34.79**	**3.72**	**0.90**	**0.49**
2. Carbon Stock Change	2.A Forests	-758.21	129.89				
	2.B Shrublands	-124.24	51.82				
	2.C Grasslands	-36.37	45.24				
	2.D Croplands	-67.89	15.47				
	2.E Wetlands	-44.71	0.40[a]				
	2.F Urban Construction	2.06	0.94				
	2.G Burial	-73.33	36.67				
	2.H Wood Products	-103.07	10.46				
	Subtotal	**-1205.76**	**152.64**				
	NBP	-978.94	316.76				
	Land Cover and Land Use Change	-290.17	281.72				
	Subtotal	**-1269.10**	**423.92**				
3. Lateral Adjustments	3.A Net Trade	-194.33	38.87				
	3.B Lateral Transport to Ocean	-150.30	30.06				
	3.C Fossil Fuel RCC	322.67	18.33				
	3.D Biogenic RCC	135.67	66.00				
4. Agriculture	4.A Enteric Fermentation			9.60	1.34		
	4.B Manure			1.91	0.92	0.30	0.11

	Management						
	4.C Agricultural Soil			9.26	2.82	0.80	0.26
	4.D Aquaculture	54.93	21.00	2.93	1.07	0.07	0.05
	Subtotal			**23.70**	**3.43**	**1.17**	**0.29**
5. Other Sectors	5.A Wetlands			3.46	0.50		
	5.B Natural Soil			-2.62	0.26	0.78	0.09
	5.C Fires	84.36	12.56	0.28	0.03	0.01	0.00
	5.D Inland Waters	348.40	146.66	4.09	1.77	0.04	0.03
	5.E Termites			0.32			
	Subtotal			**5.53**	**1.86**	**0.83**	**0.09**
	5.H Geological Seepage[b]			2.17	0.43		
	TD Inversion	-1515.33	450.08	30.98	7.52	2.24	0.61
Balance	**BU Land Budget**	**-1356.06**	**155.57**	**29.23**	**3.90**	**2.00**	**0.31**
	TD Land Budget	**-1251.33**	**456.92**	**30.98**	**7.52**	**2.24**	**0.61**

[a] The uncertainty for 2.E is estimated as 21% of the mean value (NCCC, 2018).

[b] Geological seepage is not contained within the boundaries of our terrestrial ecosystem framework.

673 3.1.2 Bottom-up

674 Forests expanded rapidly since 2000 over East Asia. According to FAO, forest area
675 increased by more than 15% from 2.3×10^8 ha in 2000 to 2.7×10^8 ha in 2020, accounting for ~7%
676 of global forests. Adding up forest inventory estimates from East Asian countries, the carbon
677 stock in East Asia's forest increased by 758.2 ± 129.9 Tg CO_2 yr^{-1}, which is mostly contributed
678 by forest plantation in China (Yu et al. 2022). The forest carbon sink was largely due to
679 increasing biomass, which was reported consistently by ground forest surveys and passive
680 microwave measurements (see Methods). Shrublands, grasslands, croplands and wetlands were
681 also found to be weaker CO_2 sinks of -124.2 ± 51.8 Tg CO_2 yr^{-1}, -36.4 ± 45.2 Tg CO_2 yr^{-1}, -67.9
682 ± 15.5 Tg CO_2 yr^{-1}, -44.7 ± 0.4 Tg CO_2 yr^{-1} , respectively (Table 1). Adding up the carbon burial
683 in inland waters and the accumulated carbon in wood products (see Methods), the inventory-
684 based method estimated an East Asia's CO_2 sink of -1356.1 ± 155.6 Tg CO_2 yr^{-1}.

685 3.1.3 CO2 budget synthesis

686 It is encouraging to see the top-down and bottom-up estimates of land CO_2 sink are
687 within ±10% of one another (between -1251.3 ± 456.9 Tg CO_2 yr^{-1} and -1356.1 ± 155.7 Tg CO_2
688 yr^{-1}) during 2000s and 2010s, though both estimates were larger than the ensemble mean of Net
689 Biome Production estimated by the 18 TRENDY ecosystem models (-978.9 ± 316.8 Tg CO_2 yr^{-1})
690 (Pierre Friedlingstein et al., 2022). It should be noted that these TRENDY model estimates were

forced by varying climate and CO_2, but by constant land cover. There is emerging evidence from forest inventories, remote sensing and process-based and book-keeping models that land cover and land use change flux (Fluc) in East Asia is a strong net sink of atmospheric CO_2 (e.g., Piao et al. 2018, Yu et al. 2022, Leng et al. under review). Based on our synthesis , we estimated that Fluc over East Asia as a sink of -290.2 Tg CO_2 yr^{-1}. Adding TRENDY model NBP and this Fluc, the resulting land CO_2 sink estimate was -1269.1 ± 423.9 Tg CO_2 yr^{-1}, close to both the top-down and bottom-up estimates.

We also noted that uncertainties associated with Fluc remain large for East Asia. When forced with varying land cover, all TRENDY models estimated Fluc over East Asia as a net source of CO_2 of more than 100 Tg C yr^{-1} (Figure 3). Such issue also occurred in estimates from Hansis et al. (2015). This is probably because both TRENDY models and Hansis et al. (2015) were driven by a common land use forcing LUH2 (Chini et al., 2021) which reported increasing cropland area and decreasing forest area over East Asia, which contradicts the evidence from ground and satellite observations (e.g., Piao et al. 2018, Yu et al. 2022, Leng et al. under review).

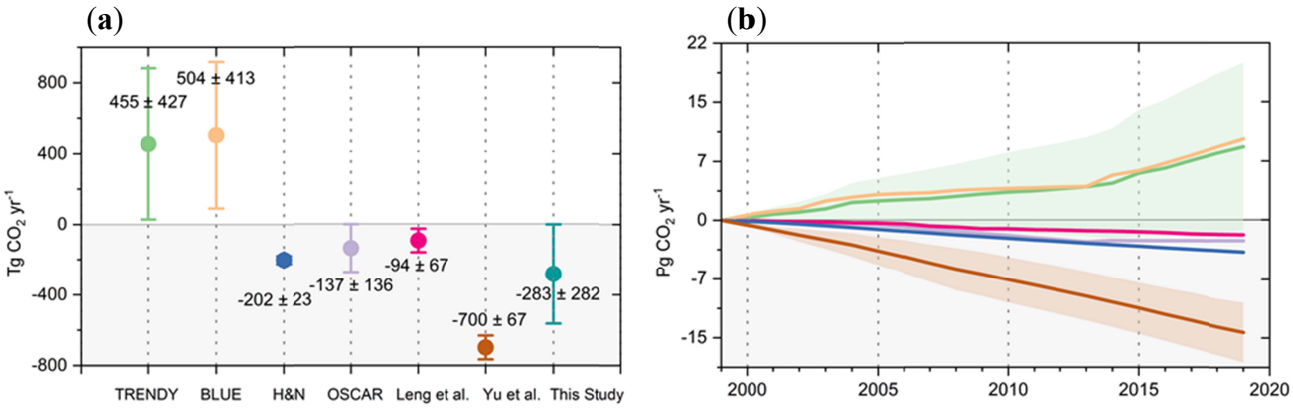

Figure 3. Comparison of different estimates on flux of land cover and land use change (Fluc) in East Asia. (**a**) Different Fluc estimates over East Asia; (**b**) Cumulative Fluc over EA from 2000-2019.

The land CO_2 sink over East Asia contributes more than one sixth of the global land CO_2 sink (Pierre Friedlingstein et al., 2022), which means its CO_2 sink per area is stronger than the global average. However, the sink offsets fossil fuel emissions of East Asia by less than 15% (Pierre Friedlingstein et al., 2022). It implies that even tripling the land CO_2 sink over East Asia, will still not satisfy carbon neutrality ambitions of East Asian countries. Thus, a realistic pathway of carbon neutrality would have to combine both CO_2 emission reduction and CO_2 sink enhancement.

3.2 CH_4 budget

3.2.1 Top-down

There are ten atmospheric inversion models for estimating CH_4 fluxes over East Asia, which yielded the CH_4 emission from terrestrial ecosystems as 31.0 ±7.5 Tg CH_4 yr^{-1} (Table 1) for the decades of 2000s and 2010s, after adjusting for fossil fuel, waste and landfill emissions and geological seepage (see Methods). The global CH_4 inversion models provided by Global

Carbon Project (Saunois et al., 2020) basically used the same set of observations reporting on the range from 26.1 Tg CH_4 yr^{-1} to 38.2 Tg CH_4 yr^{-1}, while the regional inversion by Zhang et al. (2022) using seven additional sites over China reported 30.6 Tg CH_4 yr^{-1} which is also within the range of the global inversions. These results were also consistent with Thompson et al. (2015), whose inversion used CH_4 and its isotope measurements with a nested grid over East Asia.

3.2.2 Bottom-up

The CH_4 fluxes can be broadly classified into two sectors (Figure 2), the agricultural sector (enteric fermentation, manure management, paddy croplands and freshwater aquaculture) and the natural ecosystem sector (wetlands, lake, ponds and other inland water bodies, wild fires, termites, and soil uptake).

For the agricultural sector, the largest flux term was found to be the enteric fermentation in ruminant animals (9.6 ± 1.3 Tg CH_4 yr^{-1}). Although traditional meat sources of East Asian countries are swine and poultries (chickens and ducks), there is a growing consumption of beef and lamb. If such tendency persists, the local production could become the dominant source of CH_4 emission in this region, though the per capita consumption of beef and lamb over East Asia are still below the global average (FAO, 2022). One of the collateral consequences of both ruminant animals and swine and chickens is CH_4 emission from manure management, which amounts to 1.9 ± 0.9 Tg CH_4 yr^{-1}. Another large flux term is CH_4 emission from paddy rice fields (9.3 ± 2.8 Tg CH_4 yr^{-1}). Since rice is the primary staple food for China, Japan, South Korea and North Korea, East Asia contains ~20% of global rice croplands (Figure 1), the majority of which is flooded and more productive than the global average. Thus, it is not surprising that about one third of the global CH_4 emission from paddy rice fields comes from the East Asia region (Saunois et al. 2020). Another smaller but significant flux is CH_4 emission from freshwater aquaculture (2.9 ± 1.1 Tg CH_4 yr^{-1}), because more than 60% of the global freshwater aquaculture products comes from East Asia, in particular China (FAO 2021, Yuan et al. 2019, Zhou et al. 2021). Overall, the agricultural sector emits 23.7 ± 3.4 Tg CH_4 yr^{-1} (Table 1).

For natural ecosystems, the largest sources were wetlands and inland water bodies (lakes, ponds and reservoirs), which we estimated as 3.5 ± 0.5 Tg CH_4 yr^{-1} and 4.1 ± 1.8 Tg CH_4 yr^{-1}, respectively, according to several global and regional studies (see Methods). The ensemble of 13 wetland models estimated a large range of CH_4 emission from 0.8 ± 0.2 to 10.4 ± 0.5 Tg CH_4 yr^{-1}. The wetland CH_4 emission over East Asia only contributes less than 2% of global wetland CH_4 emission (Saunois et al. 2020), partly because the small fraction of global wetland area (~4%), according to global dataset of Wetland Area and Dynamics for Methane Modeling (WAD2M; Z. Zhang et al. (2021)). The sink of CH_4 by non-saturated oxygenated soil is the primary land sink, which was estimated as -2.6 ± 0.3 Tg CH_4 yr^{-1} over East Asia, whose global contribution is commeasurable to its land fraction. CH_4 emissions from wild fires (0.3 ± 0.1 Tg CH_4 yr^{-1}) and termites (~0.3 Tg CH_4 yr^{-1}) were relatively small over East Asia. All added together, natural ecosystems emit 5.5 ± 1.9 Tg CH_4 yr^{-1} (Table 1).

3.2.3 CH4 Budget Synthesis

It appears encouraging to find the bottom-up estimates of land CH_4 emission over East Asia (29.2 ± 3.9 Tg CH_4 yr^{-1}) to be close (< ±5% for ensemble means) to the top-down estimates of the land CH_4 emission (31.0 ± 7.5 Tg CH_4 yr^{-1}). However, this could be in part coincident given the large uncertainties in some major flux terms, as the variation within BU ensembles and

765 within TD ensembles is larger than their difference. For example, the challenge to estimate CH_4
766 ebullition from inland waters remain a major source of uncertainties for inland water CH_4
767 emissions that studies may differ by one order of magnitude (e.g., Chen et al. 2013, Stavert et al.
768 2021). The agricultural sector is the dominant sources of land CH_4 emission, whose magnitudes
769 was three times more than the CH_4 emissions from natural ecosystems. The high intensity of rice
770 cultivation and inland water aquaculture has made East Asia's contribution to global land CH_4
771 emission larger than its land fraction (~8%). Unlike CO2, the magnitude of anthropogenic CH4
772 emissions from fossil fuel combustion and waste and landfill has a similar magnitude (34.8 ± 3.7
773 Tg CH_4 yr^{-1}) to land CH4 emissions at the same period (Table 1).

774 ## 3.3 N_2O budget

775 ### 3.3.1 Top-down

776 The four atmospheric inversion models reported an average estimate of land N_2O
777 emissions over East Asia of 2.2 ± 0.6 Tg N_2O yr^{-1} during 2000s and 2010s, with individual
778 estimates ranging from 1.4 Tg N_2O yr^{-1} to 3.1 Tg N_2O yr^{-1}. Compared with CO_2 and CH_4, the
779 available N_2O observation sites remain scarce globally (Thompson et al., 2019), and only few
780 sites were distributed in or around East Asia. Therefore, the smaller relative uncertainties among
781 the N_2O inversion models should be treated with caution, since the estimates were poorly
782 constrained by regional observations, and the uncertainties associated with different sets of
783 observations were not considered in this model ensemble. For similar reasons, the hotspots of the
784 N_2O emissions should come mostly from the prior flux pattern (Figure 5), rather than
785 observation constraints.

786 ### 3.3.2 Bottom-up

787 The land N_2O emissions could also be classified into two general categories (Figure 2),
788 the agricultural sector (manure management, cropland, and freshwater aquaculture) and the
789 natural ecosystem sector (natural soils, wild fires, and inland water bodies).

790 The cropland N_2O emission was found to be the largest flux at 0.8 ± 0.3 Tg N_2O yr^{-1}
791 (Table 1). It contributes to about one fifth of global cropland N_2O emission (Q. Wang et al.,
792 2020), which is due to the excessive nitrogen fertilizer input in some East Asian countries (e.g.,
793 Yu et al. 2019). We estimated the second largest emission source to be from manure
794 management (0.3 ± 0.1 Tg N_2O yr^{-1}), with individual estimates by inventories or process-based
795 models differing by five times from 0.1 Tg N_2O yr^{-1} to 0.5 Tg N_2O yr^{-1} (see Methods). The lack
796 of spatially explicit data of storage duration and treatment type for livestock dung and urine
797 could be responsible for the large uncertainties, as well as the potential biases of the fraction of
798 total nitrogen excretion by livestock species/categories and manure management system and the
799 associated emission factors (Xiaoqing Cui et al., 2021). The freshwater aquaculture is also a non-
800 negligible N_2O emission source (0.1 ± 0.1 Tg N_2O yr^{-1}), given much more intense nitrogen input
801 into these fish/shrimp/crab farms than the other inland water bodies and its wide distribution over
802 East Asia, in particular over China (Yuan et al., 2019). Because N_2O emission estimates for
803 freshwater aquaculture were mostly available over China, we had to use all available Chinese
804 estimates and only one available Japanese estimate to represent the East Asia. This should lead to
805 a minor underestimate given the small ratio (<5%; FAO, 2022) of contributions of other
806 countries to the East Asian freshwater aquaculture production.

On the natural sector, natural soil emission was found to be the predominant source (0.8 ± 0.1 Tg N_2O yr^{-1}), according to the VISIT model (Ito et al. 2019). Apparently, although nitrogen deposition over East Asia is much higher than the global average (e.g., Yu et al. 2019b), its contribution to global natural soil N_2O emission (Tian et al. 2020) is sizeable to or even smaller than East Asian land fraction due to large dryland area in its western part. The sum of wild fires and inland water N_2O emissions were less than 0.1 Tg N_2O yr^{-1} (Table 1), resulting in a synthesized natural sector N_2O emission estimates of 0.8 ± 0.1 Tg N_2O yr^{-1}.

3.3.3 N2O Budget Synthesis

Overall, we found the bottom-up estimate of land N_2O emissions over East Asia was 2.0 ± 0.3 Tg N_2O yr^{-1}, while the top-down estimate was 2.2 ± 0.6 Tg N_2O yr^{-1}. This regional source of N_2O contributes to more than 30% of global land N_2O emission (Tian et al. 2020), highlighting East Asia as the global hotspot region for curbing N_2O emissions. Among the flux terms, the agricultural sector accounted for more than 60% of all N_2O emissions, despite the fact that croplands only occupy less than 20% of the land area. The land N_2O emissions over East Asia was two times than the anthropogenic N2O emission from fossil fuel combustion and waste and landfill (9.0 ± 0.5 Tg N_2O yr^{-1}) for the same period (Table 1). Compared with CO_2 and CH_4, the consistency of N_2O emission between the top-down and bottom-up estimates were the poorest (>10%), reflecting the larger uncertainties in assessing the more potent greenhouse gas, both for the top-down and for the bottom-up estimates. Unlike CO_2 and CH_4, there is no direct satellite N_2O measurements to be used for atmospheric inversion (Shen et al. in review). Considering also the fewest available measurement sites, there is an urgent need for increasing the number of N_2O observation sites. In addition, the inventory-based estimates also vary by 3-5 times at country/regional scales, highlighting the need to further develop spatial representation of agricultural management practices (e.g., fertilization, irrigation, tillage, manure storage and treatment) and the emission factors, which would also support the development of mitigation strategies to address nitrogen pollutions in air and waters (e.g., Gu et al. 2023) .

3.4 Greenhouse gas synthesis

We used greenhouse gas warming potential (GWP) on the 100-year time horizon (IPCC, 2021; Table S1) to account for varying impacts of the three greenhouse gases in our assessment on the overall GHG gas balance of the region and impacts on the global climate system. The net source of CH_4 was estimated at 836.5 ± 203.1 Tg CO_2eq yr^{-1} by the top-down approach and at 789.2 ± 105.3 Tg CO_2eq yr^{-1} by the bottom-up approach. The net source of N_2O was estimated as 611.7 ± 166.4 Tg CO_2eq yr^{-1} by the top-down approach and 546.1 ± 83.4 Tg CO_2eq yr^{-1} by the bottom-up approach. In either approach, the net sources of CH_4 and N_2O exceeded the net sink of CO_2 (-1251.3 ± 456.9 Tg CO_2 yr^{-1} by the top-down and -1356.1 ± 155.6 Tg CO_2 yr^{-1}), rendering the land over East Asia a net source of greenhouse gases (196.9 ± 527.0 Tg CO_2eq yr^{-1} by the top-down and -20.8 ± 205.5 Tg CO_2eq yr^{-1} by the bottom-up) (Figure 4; Table 2). GHG balance based on GWP on the 20-year time horizon was also calculated (Table 2), the overall source is substantially stronger due to the much higher weight of short-lived CH4, emphasizing the challenge of developing sustainable technical approaches to reduce CH4 emissions without compromising the agricultural demand. No matter for the 100-year or 20-year horizon, the climate mitigation effects of the CO_2 uptake by terrestrial ecosystems in the East Asia region could have been exceeded by its net release of CH_4 and N_2O into the atmosphere.

850

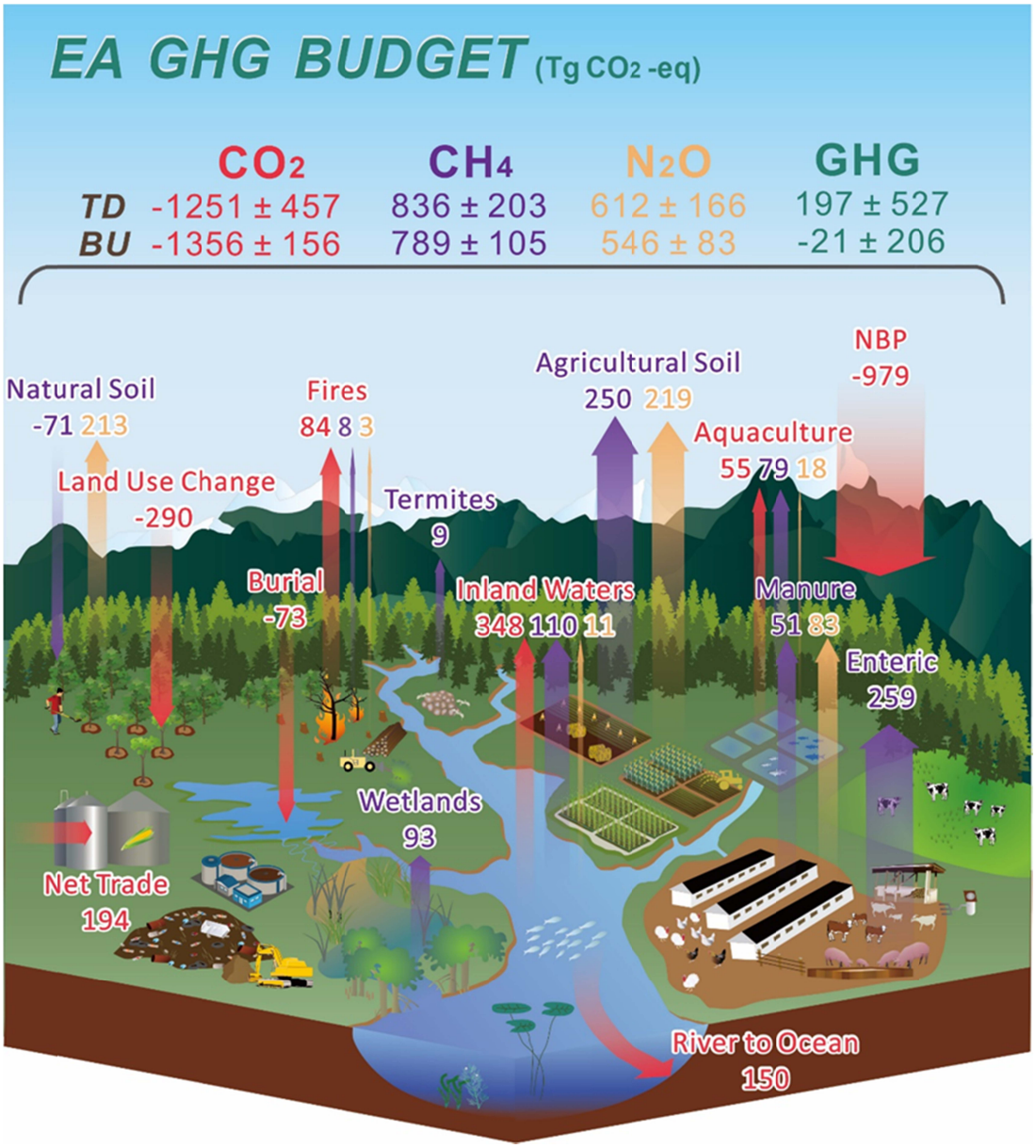

851 **Figure 4**. East Asia greenhouse gas (GHG) budget during 2000s and 2010s. The color arrows
852 represent GHG fluxes (in Tg CO_2eq yr^{-1} for 2000–2019**)** as follows: red, CO_2; purple, CH_4;
853 yellow, N_2O. Definitions and explanations of the flux terms can be found in the Methods section.

854 **Table 2**. Terrestrial GHG budget based on GWP100 and GWP20 metrics.

Terrestrial GHG budget (Tg CO_2eq yr^{-1})	**CO_2**		**CH_4**		**N_2O**		**GHG total**		**P1**[a]	**P2**[b]
	Mean	**sd**	**Mean**	**sd**	**Mean**	**sd**	**Mean**	**sd**		
GWP100										

TD	-1251.3	456.9	836.5	203.1	611.7	166.4	196.9	527.0	116%	823%
BU	-1356.1	155.6	789.2	105.3	546.1	83.4	-20.8	205.5	98%	760%
Natural	-1288.2	154.8	149.3	50.1	226.8	25.3	-912.1	164.7	29%	
Agricultural	-67.9	15.5	639.9	92.6	319.3	79.5	891.3	123.0	1413%	
GWP20										
TD	-1251.3	456.9	2469.2	599.4	611.7	166.4	1829.6	771.8	246%	823%
BU	-1356.1	155.6	2329.7	310.8	546.1	83.4	1519.7	357.4	212%	760%
Natural	-1288.2	154.8	440.8	147.9	226.7	25.3	-620.7	215.6	52%	
Agricultural	-67.9	15.5	1888.9	273.4	319.3	79.5	2140.4	285.1	3253%	

[a] Proportion of land CO_2 sink being offset by terrestrial GHG source

[b] Proportion of land CO_2 sink being offset by total fossil fuel source

When we separated the land ecosystems into agricultural ecosystems and natural ecosystems, which was only possible in bottom-up approach, we found that the natural ecosystems over East Asia were a significant net GHG sink (-912.1 ± 164.7 Tg CO_2eq yr^{-1}), which was offset by the net GHG source of agricultural ecosystems (891.3 ± 123.0 Tg CO_2eq yr^{-1}). This was also consistent with the location of hotspots of CH_4 and N_2O emissions, and thus net GHG emission, over areas dominated by cropland, such as the North China Plain (the region's wheat basket with widespread wheat-maize rotated croplands) and southern China (rice cultivated for two or three seasons) (Figure 5). These results highlighted that the agricultural sector as the priority for climate change mitigation in terrestrial ecosystems.

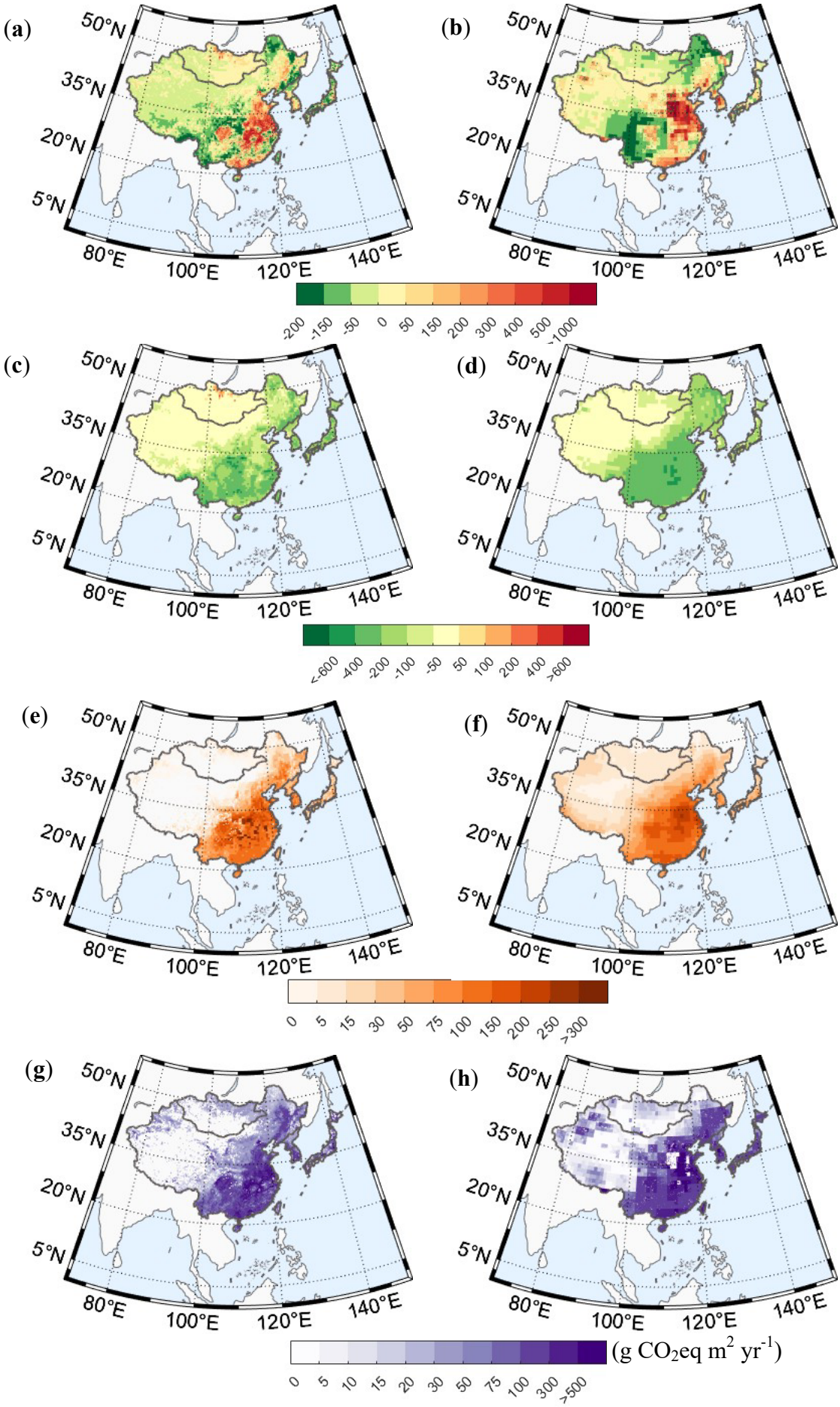
(a)
(b)
(c)
(d)
(e)
(f)
(g)
(h)
50°N
35°N
20°N
5°N
80°E
100°E
120°E
140°E
-200 -150 -50 0 50 150 200 300 400 500 >1000
<-600 -400 -200 -100 -50 50 100 200 400 >600
0 5 15 30 50 75 100 150 200 250 >300
0 5 10 15 20 30 50 75 100 300 >500
(g CO2eq m2 yr-1)

864

Figure 5. Spatial pattern of greenhouse gas (GHG) balance. (**a**) GHG balance estimated by the bottom-up approach; (**b**) GHG balance estimated by the top-down approach; (**c**) Net Biome Production simulated by dynamic global vegetation models; (**d**) CO_2 balance estimated by the atmospheric inversions; (**e**) CH_4 balance estimated by the inventory-based approach; (**f**) CH_4 balance estimated by the atmospheric inversions; (**g**) N_2O emission estimated by the inventory-based approach; (**h**) N_2O budget balance estimated by the atmospheric inversions (unit: g CO_2eq m^2 yr^{-1}).

Among the three GHGs, CO_2 fluxes were largest in the magnitude and uncertainties (Figure 6). Compared with the first phase of Regional Carbon Cycle Assessment Program (RECCAP-1), which demonstrated that terrestrial ecosystem over East Asia was a net CO_2 sink between -806.7 Tg CO_2 yr^{-1} (bottom-up) and -990.0 Tg CO_2 yr^{-1} (top-down) during 1990s and 2000s (S. L. Piao et al., 2012), the new estimates on East Asia's CO_2 sink appear more convergent between the bottom-up and the top-down approaches, with differences within ±20%. However, large uncertainties remain in several flux terms. For example, forest CO_2 sink contributes to more than half of the land CO_2 sink and ~75% of the uncertainties in land CO_2 sink, despite new sources of independent data emerging recently, such as forest biomass estimates from both passive satellite microwave measurements (e.g., Chang et al. 2023) and the combined LIDAR and multi-spectral optical remote sensing (e.g., Xu et al. 2021). Constraining soil carbon budget also needs additional data. CH_4 emission from the paddy fields and N_2O emission from cropland soils contribute the largest to uncertainties in CH_4 and N_2O emissions, respectively (Figure 6).

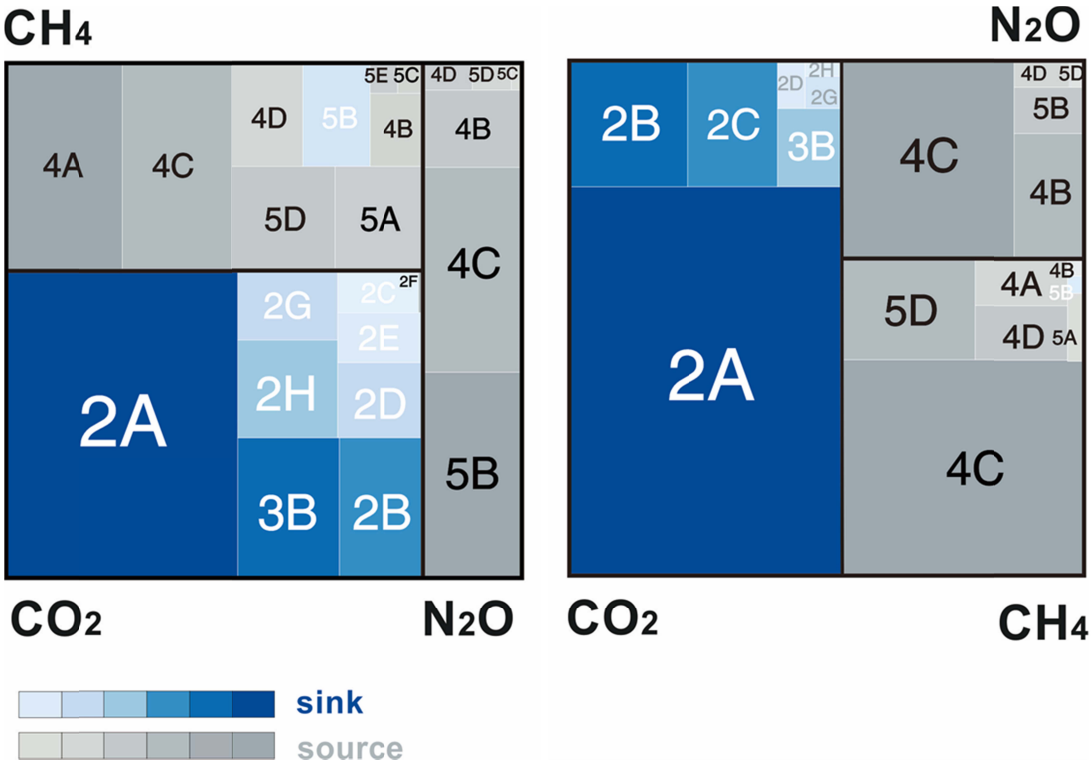

Figure 6. Contribution of major flux terms to the magnitude of greenhouse gas budgets and to the uncertainties based on GWP100. The blue block indicates the GHG sink, the gray block

indicates the GHG source. The thick black lines distinguish the three gases. (left) Contribution of each flux term to the magnitude of GHG budgets. (right) Contribution of each flux term to the overall uncertainties.

4 Conclusions

Terrestrial ecosystems over East Asia were a net GHG source based on the dual-constraint of top-down and bottom-up approaches during 2000s and 2010s, indicating that the CO_2 sink in the ecosystems could have been fully offset by the net source of CH_4 and N_2O. Compared to the global GHG estimate from H. Tian et al. (2016), both of our top-down and bottom-up estimates indicated that CH_4 and N_2O budgets of East Asia account for ~10% of the global budget, while the corresponding proportion of CO_2 sink to the globe is more than 20% (top-down: 24.50%; bottom-up: 22.88%). The remarkable carbon sink capacity of East Asia made the overall balance of terrestrial ecosystem GHG close to neutral. While natural ecosystems were a net sink of GHG, it has been overcompensated by net sources of GHG from the agricultural ecosystems. This study highlights the agricultural sector as the priority for climate mitigation efforts on terrestrial ecosystems over East Asia. The emerging data sources, improving modelling capacities in recent years have contributed to the improved closure between top-down and bottom-up estimates, though sizeable uncertainties remain in some major flux terms, such as land use change. Future studies should need to further refine emission factors and activity data to provide estimates with better spatial and temporal resolutions, which would not only facilitate the policy making for climate change mitigation, but also serve monitoring the progresses in achieving climate neutrality.

Acknowledgments

This study was supported by National Natural Science Foundation of China (No. 42171096) and Ministry of Science and Technology of People's Republic of China (No. 2019YFA0607302). Ronny Lauerwald acknowledges funding from French state aid, managed by ANR under the "Investissements d'avenir" programme (ANR-16-CONV-0003). The updated CO_2 and CH_4 inversions using MIROC4-ACTM are prepared by Naveen Chandra and Dmitry Belikov, respectively. Patra Prabir is partly supported by the Arctic Challenge for Sustainability phase II (ArCS-II; JPMXD1420318865) and Environment Research and Technology Development Fund (SII8; JPMEERF21S20800), Government of Japan. Net CO2 flux estimates from the University of Edinburgh are provided by Liang Feng and Paul Palmer who acknowledge funding from the UK National Centre for Earth Observation (NE/R016518/1). We thank Dr. Ingrid Luijkx for providing atmospheric CO2 inversions and suggestions to the manuscript. The PyVAR-CAMS modelling results were funded through the Copernicus Atmosphere Monitoring Service implemented by ECMWF on behalf of the European Commission, and were generated using computing resources from LSCE.

References

Allen, G. H., & Pavelsky, T. M. (2018). Global extent of rivers and streams. *Science, 361*(6402), 585-588. doi:10.1126/science.aat0636

Arjo, S., Janot, T., & Sander, H. (2020). Description of the CH4 inversion production chain 2020 (CAMS73_2018SC3_D73.5.2.2-2020_202012_production_chain_v1).

930 Bastos, A., Ciais, P., Sitch, S., Aragão, L. E. O. C., Chevallier, F., Fawcett, D., et al. (2022). On
931 the use of Earth Observation to support estimates of national greenhouse gas emissions
932 and sinks for the Global stocktake process: lessons learned from ESA-CCI RECCAP2.
933 *Carbon Balance and Management, 17*(1), 15. doi:10.1186/s13021-022-00214-w
934 Bloom, A. A., Bowman, K. W., Lee, M., Turner, A. J., Schroeder, R., Worden, J. R., et al.
935 (2017). A global wetland methane emissions and uncertainty dataset for atmospheric
936 chemical transport models (WetCHARTs version 1.0). *Geoscientific Model Development,*
937 *10*(6), 2141-2156. doi:10.5194/gmd-10-2141-2017
938 Bouwman, A. F. (1996). Direct emission of nitrous oxide from agricultural soils. *Nutrient*
939 *Cycling in Agroecosystems, 46*(1), 53-70. doi:10.1007/BF00210224
940 Canadell, J. G., Monteiro, P. M., Costa, M. H., Da Cunha, L. C., Cox, P. M., Alexey, V., et al.
941 (2021). Global carbon and other biogeochemical cycles and feedbacks. IPCC AR6 WGI,
942 Final Government Distribution, chapter 5.doi:10.1017/9781009157896.007
943 Caro, D., Davis, S. J., Bastianoni, S., & Caldeira, K. (2014). Global and regional trends in
944 greenhouse gas emissions from livestock. *Climatic Change, 126*(1-2), 203-216.
945 doi:10.1007/s10584-014-1197-x
946 Chandra, N., Patra, P. K., Bisht, J. S. H., Ito, A., Umezawa, T., Saigusa, N., et al. (2021).
947 Emissions from the Oil and Gas Sectors, Coal Mining and Ruminant Farming Drive
948 Methane Growth over the Past Three Decades. *Journal of the Meteorological Society of*
949 *Japan. Ser. II, advpub*. doi:10.2151/jmsj.2021-015
950 Chandra, N., Patra, P. K., Niwa, Y., Ito, A., Iida, Y., Goto, D., et al. (2022). Estimated regional
951 CO2 flux and uncertainty based on an ensemble of atmospheric CO2 inversions. *Atmos.*
952 *Chem. Phys., 22*(14), 9215-9243. doi:10.5194/acp-22-9215-2022
953 Chang, Z., Fan, L., Wigneron, J.-P., Wang, Y.-P., Ciais, P., Chave, J., et al. (2023). Estimating
954 Aboveground Carbon Dynamic of China Using Optical and Microwave Remote-Sensing
955 Datasets from 2013 to 2019. *Journal of Remote Sensing, 3*, 0005.
956 doi:10.34133/remotesensing.0005
957 Chen, B., Zhang, H., Wang, T., & Zhang, X. (2021). An atmospheric perspective on the carbon
958 budgets of terrestrial ecosystems in China: progress and challenges. *Science Bulletin,*
959 *66*(17), 1713-1718. doi:10.1016/j.scib.2021.05.017
960 Chen, C., Park, T., Wang, X., Piao, S., Xu, B., Chaturvedi, R. K., et al. (2019). China and India
961 lead in greening of the world through land-use management. *Nature Sustainability, 2*(2),
962 122-129. doi:10.1038/s41893-019-0220-7
963 Chen, H., Zhu, Q., Peng, C., Wu, N., Wang, Y., Fang, X., et al. (2013). Methane emissions from
964 rice paddies natural wetlands, and lakes in China: synthesis and new estimate. *Glob*
965 *Chang Biol, 19*(1), 19-32. doi:10.1111/gcb.12034
966 Chevallier, F., Fisher, M., Peylin, P., Serrar, S., Bousquet, P., Bréon, F.-M., et al. (2005).
967 Inferring CO2 sources and sinks from satellite observations: Method and application to
968 TOVS data. *Journal of Geophysical Research: Atmospheres, 110*(D24).
969 doi:10.1029/2005JD006390
970 Chini, L., Hurtt, G., Sahajpal, R., Frolking, S., Klein Goldewijk, K., Sitch, S., et al. (2021).
971 Land-use harmonization datasets for annual global carbon budgets. *Earth System Science*
972 *Data, 13*(8), 4175-4189. doi:10.5194/essd-13-4175-2021
973 Choi, S.-D., & Chang, Y.-S. (2004). Factors Affecting the Distribution of the Rate of Carbon
974 Uptake by Forests in South Korea. *Environmental Science & Technology, 38*(2), 484-
975 488. doi:10.1021/es034533u

Ciais, P., Bastos, A., Chevallier, F., Lauerwald, R., Poulter, B., Canadell, P., et al. (2022). Definitions and methods to estimate regional land carbon fluxes for the second phase of the REgional Carbon Cycle Assessment and Processes Project (RECCAP-2). *Geoscientific Model Development*. doi:10.5194/gmd-2020-259

Ciais, P., Tan, J., Wang, X., Roedenbeck, C., Chevallier, F., Piao, S. L., et al. (2019). Five decades of northern land carbon uptake revealed by the interhemispheric CO(2) gradient. *Nature, 568*(7751), 221-225. doi:10.1038/s41586-019-1078-6

Crippa, M., Guizzardi, D., Banja, M., Solazzo, E., Muntean, M., Schaaf, E., et al. (2022). CO2 emissions of all world countries. *JRC/IEA/PBL 2022 Report, EUR 31182 EN, Publications Office of the European Union, Luxembourg*. doi:10.2760/730164

Cui, X., Shang, Z., Xia, L., Xu, R., Adalibieke, W., Zhan, X., et al. (2022). Deceleration of Cropland-N2O Emissions in China and Future Mitigation Potentials. *Environmental Science & Technology, 56*(7), 4665-4675. doi:10.1021/acs.est.1c07276

Cui, X., Zhou, F., Ciais, P., Davidson, E. A., Tubiello, F. N., Niu, X., et al. (2021). Global mapping of crop-specific emission factors highlights hotspots of nitrous oxide mitigation. *Nature Food*. doi:10.1038/s43016-021-00384-9

Dong, B., Xi, Y., Cui, Y., & Peng, S. (2023). Quantifying Methane Emissions from Aquaculture Ponds in China. *Environmental Science & Technology, 57*(4), 1576-1583. doi:10.1021/acs.est.2c05218

Fang, J., Chen, A., Peng, C., Zhao, S., & Ci, L. (2001). Changes in Forest Biomass Carbon Storage in China Between 1949 and 1998. *Science, 292*(5525), 2320-2322. doi:10.1126/science.1058629

Fang, J., Liu, G., & Xu, S. (1996). Biomass and net production of forest vegetation in China. . *Acta Ecologica Sinica, 16*, 497-508.

Fang, J., Oikawa, T., Kato, T., Mo, W., & Wang, Z. (2005). Biomass carbon accumulation by Japan's forests from 1947 to 1995. *Global Biogeochemical Cycles, 19*(2). doi:10.1029/2004GB002253

Fang, J., Yu, G., Liu, L., Hu, S., & Chapin, F. S. (2018). Climate change, human impacts, and carbon sequestration in China. *Proceedings of the National Academy of Sciences, 115*(16), 4015-4020. doi:10.1073/pnas.1700304115

FAO. (2021). Emissions from agriculture and forest land. Global, regional and country trends 1990–2019. *FAOSTAT Analytical Brief Series, 25*.

Feng, L., Palmer, P. I., Parker, R. J., Deutscher, N. M., Feist, D. G., Kivi, R., et al. (2016). Estimates of European uptake of CO 2 inferred from GOSAT X CO 2 retrievals: sensitivity to measurement bias inside and outside Europe. *Atmospheric Chemistry and Physics, 16*(3), 1289-1302. doi:10.5194/acp-16-1289-2016

Friedlingstein, P., Jones, M. W., O'Sullivan, M., Andrew, R. M., Bakker, D. C. E., Hauck, J., et al. (2022). Global Carbon Budget 2021. *Earth Syst. Sci. Data, 14*(4), 1917-2005. doi:10.5194/essd-14-1917-2022

Friedlingstein, P., O'Sullivan, M., Jones, M. W., Andrew, R. M., Gregor, L., Hauck, J., et al. (2022). Global Carbon Budget 2022. *Earth System Science Data, 14*(11), 4811-4900. doi:10.5194/essd-14-4811-2022

Gasser, T., Crepin, L., Quilcaille, Y., Houghton, R. A., Ciais, P., & Obersteiner, M. (2020). Historical CO2 emissions from land use and land cover change and their uncertainty. *Biogeosciences, 17*(15), 4075-4101. doi:10.5194/bg-17-4075-2020

1021 Gilfillan, D., & Marland, G. (2021). CDIAC-FF: global and national CO2 emissions from fossil
1022 fuel combustion and cement manufacture: 1751–2017. *Earth Syst. Sci. Data, 13*(4), 1667-
1023 1680. doi:10.5194/essd-13-1667-2021
1024 *GRiSP (Global Rice Science Partnership) Rice Almanac.* (2013). (4th ed.): International Rice
1025 Research Institute, Los Baños.
1026 Gu, B., Zhang, X., Lam, S. K., Yu, Y., van Grinsven, H. J. M., Zhang, S., et al. (2023). Cost-
1027 effective mitigation of nitrogen pollution from global croplands. *Nature, 613*(7942), 77-
1028 84. doi:10.1038/s41586-022-05481-8
1029 Gütschow, J., Günther, A., & Pflüger, M. (2021). *The PRIMAP-hist national historical emissions*
1030 *time series (1750-2019) v2.3.1 (2.3.1)* doi:10.5281/zenodo.4479171
1031 Gütschow, J., Jeffery, M. L., Gieseke, R., Gebel, R., Stevens, D., Krapp, M., & Rocha, M.
1032 (2016). The PRIMAP-hist national historical emissions time series. *Earth System Science*
1033 *Data, 8*(2), 571-603. doi:10.5194/essd-8-571-2016
1034 Hansis, E., Davis, S. J., & Pongratz, J. (2015). Relevance of methodological choices for
1035 accounting of land use change carbon fluxes. *Global Biogeochemical Cycles, 29*(8),
1036 1230-1246. doi:10.1002/2014gb004997
1037 Hartmann, J., Jansen, N., Dürr, H. H., Kempe, S., & Köhler, P. (2009). Global CO2-consumption
1038 by chemical weathering: What is the contribution of highly active weathering regions?
1039 *Global and Planetary Change, 69*(4), 185-194. doi:10.1016/j.gloplacha.2009.07.007
1040 Hayashi, K., Shibata, H., Oita, A., Nishina, K., Ito, A., Katagiri, K., et al. (2021). Nitrogen
1041 budgets in Japan from 2000 to 2015: Decreasing trend of nitrogen loss to the environment
1042 and the challenge to further reduce nitrogen waste. *Environmental Pollution, 286*,
1043 117559. doi:10.1016/j.envpol.2021.117559
1044 Hoesly, R. M., Smith, S. J., Feng, L., Klimont, Z., Janssens-Maenhout, G., Pitkanen, T., et al.
1045 (2017). Historical (1750–2014) anthropogenic emissions of reactive gases and aerosols
1046 from the Community Emissions Data System (CEDS). *Geoscientific Model Development*.
1047 doi:10.5194/gmd-2017-43
1048 Houghton, R. A. (2007). Balancing the Global Carbon Budget. *Annual Review of Earth and*
1049 *Planetary Sciences, 35*(1), 313-347. doi:10.1146/annurev.earth.35.031306.140057
1050 Houghton, R. A., & Nassikas, A. A. (2017). Global and regional fluxes of carbon from land use
1051 and land cover change 1850-2015. *Global Biogeochemical Cycles, 31*(3), 456-472.
1052 doi:10.1002/2016gb005546
1053 Hu, Z., Lee, J. W., Chandran, K., Kim, S., & Khanal, S. K. (2012). Nitrous Oxide (N2O)
1054 Emission from Aquaculture: A Review. *Environmental Science & Technology, 46*(12),
1055 6470-6480. doi:10.1021/es300110x
1056 IPCC. (2006). Intergovernmental panel on climate change (IPCC) guidelines for national
1057 greenhouse gas inventories. Volume 4. Agriculture, forestry and other land uses.
1058 Intergovernmental Panel on Climate Change.https://www.ipcc-
1059 nggip.iges.or.jp/public/2006gl/vol4.html.
1060 IPCC. (2019). Intergovernmental panel on climate change (IPCC) guidelines for national
1061 greenhouse gas inventories. Volume 4. Agriculture, forestry and other land uses.
1062 Intergovernmental Panel on Climate Change.https://www.ipcc-
1063 nggip.iges.or.jp/public/2019rf/vol4.html.
1064 IPCC. (2021). Summary for policymakers. In Climate change 2021: The physical science basis.
1065 Contribution of Working Group I to the Sixth Assessment Report of the

Intergovernmental Panel on Climate Change.https://www.ipcc.ch/report/ar6/wg1/chapter/summary-for-policymakers/.

IPCC. (2022). In P. R. Shukla, J. Skea, R. Slade, A. Al Khourdajie, R. van Diemen, D. McCollum, M. Pathak, S. Some, P. Vyas, R. Fradera, M. Belkacemi, A. Hasija, G. Lisboa, S. Luz, & J. Malley (Eds.), Climate change 2022: Mitigation of climate change. Contribution of working group III to the sixth assessment report of the intergovernmental panel on climate change. Cambridge University Press. https://doi.org/10.1017/9781009157926.

Ito, A., Nishina, K., Ishijima, K., Hashimoto, S., & Inatomi, M. (2018). Emissions of nitrous oxide (N2O) from soil surfaces and their historical changes in East Asia: a model-based assessment. *Progress in Earth and Planetary Science, 5*. doi:10.1186/s40645-018-0215-4

Ito, A., Tohjima, Y., Saito, T., Umezawa, T., Hajima, T., Hirata, R., et al. (2019). Methane budget of East Asia, 1990-2015: A bottom-up evaluation. *Science of the Total Environment, 676*, 40-52. doi:10.1016/j.scitotenv.2019.04.263

Janssens, I. A., Freibauer, A., Ciais, P., Smith, P., Nabuurs, G.-J., Folberth, G., et al. (2003). Europe's Terrestrial Biosphere Absorbs 7 to 12% of European Anthropogenic CO2 Emissions. *Science, 300*(5625), 1538-1542. doi:10.1126/science.1083592

Jiang, F., Chen, J. M., Zhou, L., Ju, W., Zhang, H., Machida, T., et al. (2016). A comprehensive estimate of recent carbon sinks in China using both top-down and bottom-up approaches. *Scientific Reports, 6*, 22130. doi:10.1038/srep22130

Jones, M. W., Andrew, R. M., Peters, G. P., Janssens-Maenhout, G., De-Gol, A. J., Ciais, P., et al. (2021). Gridded fossil CO2 emissions and related O2 combustion consistent with national inventories 1959–2018. *Scientific Data, 8*(1), 2. doi:10.1038/s41597-020-00779-6

Kumari, S., Fagodiya, R. K., Hiloidhari, M., Dahiya, R. P., & Kumar, A. (2020). Methane production and estimation from livestock husbandry: A mechanistic understanding and emerging mitigation options. *Sci Total Environ, 709*, 136135. doi:10.1016/j.scitotenv.2019.136135

Liu, J., Baskaran, L., Bowman, K., Schimel, D., Bloom, A. A., Parazoo, N. C., et al. (2021). Carbon monitoring system flux net biosphere exchange 2020 (CMS-flux NBE 2020). *Earth System Science Data, 13*(2), 299-330. doi:10.5194/essd-13-299-2021

Long, Y., Yoshida, Y., Zhang, H., Zheng, H., Shan, Y., & Guan, D. (2020). Japan prefectural emission accounts and socioeconomic data 2007 to 2015. *Scientific Data, 7*(1), 233. doi:10.1038/s41597-020-0571-y

Luo, Y., Keenan, T. F., & Smith, M. (2015). Predictability of the terrestrial carbon cycle. *Glob Chang Biol, 21*(5), 1737-1751. doi:10.1111/gcb.12766

Maki, T., Ikegami, M., Fujita, T., Hirahara, T., Yamada, K., Mori, K., et al. (2010). New technique to analyse global distributions of CO2 concentrations and fluxes from non-processed observational data. *Tellus B: Chemical and Physical Meteorology, 62*(5), 797-809. doi:10.1111/j.1600-0889.2010.00488.x

Mayorga, E., Seitzinger, S. P., Harrison, J. A., Dumont, E., Beusen, A. H. W., Bouwman, A. F., et al. (2010). Global Nutrient Export from WaterSheds 2 (NEWS 2): Model development and implementation. *Environmental Modelling & Software, 25*(7), 837-853. doi:10.1016/j.envsoft.2010.01.007

McDuffie, E. E., Smith, S. J., O'Rourke, P., Tibrewal, K., Venkataraman, C., Marais, E. A., et al. (2020). A global anthropogenic emission inventory of atmospheric pollutants from

sector- and fuel-specific sources (1970–2017): an application of the Community Emissions Data System (CEDS). *Earth System Science Data, 12*(4), 3413-3442. doi:10.5194/essd-12-3413-2020

Mendonça, R., Müller, R. A., Clow, D., Verpoorter, C., Raymond, P., Tranvik, L. J., & Sobek, S. (2017). Organic carbon burial in global lakes and reservoirs. *Nature Communications, 8*(1). doi:10.1038/s41467-017-01789-6

Messager, M. L., Lehner, B., Grill, G., Nedeva, I., & Schmitt, O. (2016). Estimating the volume and age of water stored in global lakes using a geo-statistical approach. *Nature Communications, 7*, 13603. doi:10.1038/ncomms13603

NCCC. (2010). The Second National Communication on Climate Change of The People's Republic of China, the People's Republic of China.

NCCC. (2018). The Third National Communication on Climate Change of The People's Republic of China, the People's Republic of China.

NIES. (2022). Greenhouse Gas Inventory Office of Japan and Ministry of the Environment, Japan (eds.), National Greenhouse Gas Inventory Report of JAPAN 2022, Center for Global Environmental Research, Earth System Division, National Institute for Environmental Studies, Japan.

Niwa, Y., Fujii, Y., Sawa, Y., Iida, Y., Ito, A., Satoh, M., et al. (2017). A 4D-Var inversion system based on the icosahedral grid model (NICAM-TM 4D-Var v1. 0)–Part 2: Optimization scheme and identical twin experiment of atmospheric CO 2 inversion. *Geoscientific Model Development, 10*(6), 2201-2219. doi:10.5194/gmd-10-2201-2017

Oita, A., Nagano, I., & Matsuda, H. (2018). Food nitrogen footprint reductions related to a balanced Japanese diet. *Ambio, 47*(3), 318-326. doi:10.1007/s13280-017-0944-4

Pan, Y., Birdsey, R. A., Fang, J., Houghton, R., Kauppi, P. E., Kurz, W. A., et al. (2011). A Large and Persistent Carbon Sink in the World's Forests. *Science, 333*(6045), 988-993. doi:10.1126/science.1201609

Peters, G. P., Davis, S. J., & Andrew, R. (2012). A synthesis of carbon in international trade. *Biogeosciences, 9*(8), 3247-3276. doi:10.5194/bg-9-3247-2012

Piao, S., Ciais, P., Friedlingstein, P., de Noblet-Ducoudré, N., Cadule, P., Viovy, N., & Wang, T. (2009). Spatiotemporal patterns of terrestrial carbon cycle during the 20th century. *Global Biogeochemical Cycles, 23*(4). doi:10.1029/2008gb003339

Piao, S., Fang, J., Ciais, P., Peylin, P., Huang, Y., Sitch, S., & Wang, T. (2009). The carbon balance of terrestrial ecosystems in China. *Nature, 458*(7241), 1009-1013. doi:10.1038/nature07944

Piao, S., He, Y., Wang, X., & Chen, F. (2022). Estimation of China's terrestrial ecosystem carbon sink: Methods, progress and prospects. *Science China Earth Sciences, 65*(4), 641-651. doi:10.1007/s11430-021-9892-6

Piao, S., Huang, M., Liu, Z., Wang, X., Ciais, P., Canadell, J. G., et al. (2018). Lower land-use emissions responsible for increased net land carbon sink during the slow warming period. *Nature Geoscience, 11*(10), 739-743. doi:10.1038/s41561-018-0204-7

Piao, S. L., Ito, A., Li, S. G., Huang, Y., Ciais, P., Wang, X. H., et al. (2012). The carbon budget of terrestrial ecosystems in East Asia over the last two decades. *Biogeosciences, 9*(9), 3571-3586. doi:10.5194/bg-9-3571-2012

Pugh, T. A. M., Lindeskog, M., Smith, B., Poulter, B., Arneth, A., Haverd, V., & Calle, L. (2019). Role of forest regrowth in global carbon sink dynamics. *Proceedings of the National Academy of Sciences, 116*(10), 4382-4387. doi:10.1073/pnas.1810512116

Qiu, J. (2009). China cuts methane emissions from rice fields. *Nature*. doi:10.1038/news.2009.833

Rödenbeck, C., Zaehle, S., Keeling, R., & Heimann, M. (2018). History of El Niño impacts on the global carbon cycle 1957–2017: A quantification from atmospheric CO2 data. *Philosophical Transactions of the Royal Society B: Biological Sciences, 373*(1760), 20170303. doi:10.1098/rstb.2017.0303

Saeki, T., & Patra, P. K. (2017). Implications of overestimated anthropogenic CO2 emissions on East Asian and global land CO2 flux inversion. *Geoscience Letters, 4*, 1-10. doi:10.1186/s40562-017-0074-7

Saunois, M., Stavert, A. R., Poulter, B., Bousquet, P., Canadell, J. G., Jackson, R. B., et al. (2020). The Global Methane Budget 2000–2017. *Earth System Science Data, 12*(3), 1561-1623. doi:10.5194/essd-12-1561-2020

Shan, Y., Guan, D., Zheng, H., Ou, J., Li, Y., Meng, J., et al. (2018). China CO2 emission accounts 1997–2015. *Scientific Data, 5*(1), 170201. doi:10.1038/sdata.2017.201

Shan, Y., Huang, Q., Guan, D., & Hubacek, K. (2020). China CO2 emission accounts 2016–2017. *Scientific Data, 7*(1), 54. doi:10.1038/s41597-020-0393-y

Stavert, A. R., Saunois, M., Canadell, J. G., Poulter, B., Jackson, R. B., Regnier, P., et al. (2021). Regional trends and drivers of the global methane budget. *Global Change Biology, 28*, 182-200. doi:10.1111/gcb.15901

Stephens, B. B., Gurney, K. R., Tans, P. P., Sweeney, C., Peters, W., Bruhwiler, L., et al. (2007). Weak Northern and Strong Tropical Land Carbon Uptake from Vertical Profiles of Atmospheric CO2. *Science, 316*(5832), 1732-1735. doi:10.1126/science.1137004

Tagesson, T., Schurgers, G., Horion, S., Ciais, P., Tian, F., Brandt, M., et al. (2020). Recent divergence in the contributions of tropical and boreal forests to the terrestrial carbon sink. *Nature ecology & evolution, 4*(2), 202-209. doi:10.1038/s41559-019-1090-0

Thompson, R. L., Lassaletta, L., Patra, P. K., Wilson, C., Wells, K. C., Gressent, A., et al. (2019). Acceleration of global N2O emissions seen from two decades of atmospheric inversion. *Nature Climate Change, 9*(12), 993-998. doi:10.1038/s41558-019-0613-7

Thompson, R. L., Stohl, A., Zhou, L. X., Dlugokencky, E., Fukuyama, Y., Tohjima, Y., et al. (2015). Methane emissions in East Asia for 2000-2011 estimated using an atmospheric Bayesian inversion. *Journal of Geophysical Research: Atmospheres, 120*(9), 4352-4369. doi:10.1002/2014jd022394

Tian, H., Lu, C., Ciais, P., Michalak, A. M., Canadell, J. G., Saikawa, E., et al. (2016). The terrestrial biosphere as a net source of greenhouse gases to the atmosphere. *Nature, 531*(7593), 225-228. doi:10.1038/nature16946

Tian, H., Xu, R., Canadell, J. G., Thompson, R. L., Winiwarter, W., Suntharalingam, P., et al. (2020). A comprehensive quantification of global nitrous oxide sources and sinks. *Nature, 586*(7828), 248-256. doi:10.1038/s41586-020-2780-0

Tian, H., Yang, J., Lu, C., Xu, R., Canadell, J. G., Jackson, R. B., et al. (2018). The Global N2O Model Intercomparison Project. *Bulletin of the American Meteorological Society, 99*(6), 1231-1251. doi:10.1175/bams-d-17-0212.1

Tubiello, F. N. (2019). Greenhouse Gas Emissions Due to Agriculture. In P. Ferranti, E. M. Berry, & J. R. Anderson (Eds.), *Encyclopedia of Food Security and Sustainability* (pp. 196-205). Oxford: Elsevier.

Van Der Laan-Luijkx, I. T., Van Der Velde, I. R., Van Der Veen, E., Tsuruta, A., Stanislawska, K., Babenhauserheide, A., et al. (2017). The CarbonTracker Data Assimilation Shell (CTDAS) v1. 0: implementation and global carbon balance 2001–2015. *Geoscientific Model Development, 10*(7), 2785-2800. doi:10.5194/gmd-10-2785-2017

van der Werf, G. R., Randerson, J. T., Giglio, L., van Leeuwen, T. T., Chen, Y., Rogers, B. M., et al. (2017). Global fire emissions estimates during 1997–2016. *Earth System Science Data, 9*(2), 697-720. doi:10.5194/essd-9-697-2017

Wang, J., Feng, L., Palmer, P. I., Liu, Y., Fang, S., Bosch, H., et al. (2020). Large Chinese land carbon sink estimated from atmospheric carbon dioxide data. *Nature, 586*(7831), 720-723. doi:10.1038/s41586-020-2849-9

Wang, Q., Zhou, F., Shang, Z., Ciais, P., Winiwarter, W., Jackson, R. B., et al. (2020). Data-driven estimates of global nitrous oxide emissions from croplands. *National Science Review, 7*(2), 441-452. doi:10.1093/nsr/nwz087

Wang, Y., Wang, X., Wang, K., Chevallier, F., Zhu, D., Lian, J., et al. (2022). The size of the land carbon sink in China. *Nature, 603*(7901), E7-E9. doi:10.1038/s41586-021-04255-y

Xu, L., Saatchi, S. S., Yang, Y., Yu, Y., Pongratz, J., Bloom, A. A., et al. (2021). Changes in global terrestrial live biomass over the 21st century. *Science Advances, 7*(27), eabe9829. doi:10.1126/sciadv.abe9829

Xu, P., Houlton, B. Z., Zheng, Y., Zhou, F., Ma, L., Li, B., et al. (2022). Policy-enabled stabilization of nitrous oxide emissions from livestock production in China over 1978–2017. *Nature Food, 3*(5), 356-366. doi:10.1038/s43016-022-00513-y

Xu, P., Liao, Y., Zheng, Y., Zhao, C., Zhang, X., Zheng, Z., & Luan, S. (2019). Northward shift of historical methane emission hotspots from the livestock sector in China and assessment of potential mitigation options. *Agricultural and Forest Meteorology, 272*, 1-11. doi:10.1016/j.agrformet.2019.03.022

Yu, C., Huang, X., Chen, H., Godfray, H. C. J., Wright, J. S., Hall, J. W., et al. (2019). Managing nitrogen to restore water quality in China. *Nature, 567*(7749), 516-520. doi:10.1038/s41586-019-1001-1

Yu, G., Jia, Y., He, N., Zhu, J., Chen, Z., Wang, Q., et al. (2019). Stabilization of atmospheric nitrogen deposition in China over the past decade. *Nature Geoscience, 12*(6), 424-429. doi:10.1038/s41561-019-0352-4

Yu, Z., Ciais, P., Piao, S., Houghton, R. A., Lu, C., Tian, H., et al. (2022). Forest expansion dominates China's land carbon sink since 1980. *Nature Communications, 13*(1). doi:10.1038/s41467-022-32961-2

Yuan, J., Xiang, J., Liu, D., Kang, H., He, T., Kim, S., et al. (2019). Rapid growth in greenhouse gas emissions from the adoption of industrial-scale aquaculture. *Nature Climate Change, 9*(4), 318-322. doi:10.1038/s41558-019-0425-9

Yue, X., Liao, H., Wang, H., Zhang, T., Unger, N., Sitch, S., et al. (2020). Pathway dependence of ecosystem responses in China to 1.5 °C global warming. *Atmospheric Chemistry and Physics, 20*(4), 2353-2366. doi:10.5194/acp-20-2353-2020

Zhang, B., Tian, H., Ren, W., Tao, B., Lu, C., Yang, J., et al. (2016). Methane emissions from global rice fields: Magnitude, spatiotemporal patterns, and environmental controls. *Global Biogeochemical Cycles, 30*(9), 1246-1263. doi:10.1002/2016gb005381

Zhang, L., Tian, H., Shi, H., Pan, S., Qin, X., Pan, N., & Dangal, S. R. S. (2021). Methane emissions from livestock in East Asia during 1961−2019. *Ecosystem Health and Sustainability, 7*(1). doi:10.1080/20964129.2021.1918024

Zhang, Y., Fang, S., Chen, J., Lin, Y., Chen, Y., Liang, R., et al. (2022). Observed changes in China's methane emissions linked to policy drivers. *Proceedings of the National Academy of Sciences, 119*(41), e2202742119. doi:10.1073/pnas.2202742119

Zhang, Y., Tang, K. W., Yang, P., Yang, H., Tong, C., Song, C., et al. (2022). Assessing carbon greenhouse gas emissions from aquaculture in China based on aquaculture system types, species, environmental conditions and management practices. *Agriculture, Ecosystems & Environment, 338*. doi:10.1016/j.agee.2022.108110

Zhang, Z., Fluet-Chouinard, E., Jensen, K., McDonald, K., Hugelius, G., Gumbricht, T., et al. (2021). Development of the global dataset of Wetland Area and Dynamics for Methane Modeling (WAD2M). *Earth System Science Data, 13*(5), 2001-2023. doi:10.5194/essd-13-2001-2021

Zhou, Y., Huang, M., Tian, H., Xu, R., Ge, J., Yang, X., et al. (2021). Four decades of nitrous oxide emission from Chinese aquaculture underscores the urgency and opportunity for climate change mitigation. *Environmental Research Letters, 16*(11). doi:10.1088/1748-9326/ac3177